

1 **MitoEAGLE preprint 2017-09-21(02).**

2 **The protonmotive force and respiratory control:**

3 **Building blocks of mitochondrial physiology**

4 **Part 1.**

5 http://www.mitoeagle.org/index.php/MitoEAGLE_preprint_2017-09-21

6 Preprint version 02 (2017-09-22)

7
8 **MitoEAGLE Network**

9 Corresponding author: Gnaiger E

10 Contributing co-authors

11 Ahn B, Alves MG, Beard DA, Ben-Shachar D, Bishop D, Breton S, Brown GC, Brown RA,
12 Buettner GR, Cervinkova Z, Chicco AJ, Coen PM, Collins JL, Crisóstomo L, Davis MS, Dias
13 T, Doerrier C, Ehinger J, Elmer E, Fell DA, Filipovska A, Fisher J, Garcia-Roves PM,
14 Garcia-Souza LF, Genova ML, Gonzalo H, Goodpaster BH, Han J, Harrison DK, Hellgren
15 KT, Hernansanz P, Holland O, Hoppel CL, Iglesias-Gonzalez J, Irving BA, Iyer S, Jansen-
16 Dürr P, Jespersen NR, Jha RK, Käämbre T, Kane DA, Kappler L, Keijer J, Komlodi T, Kuang
17 J, Labieniec-Watala M, Laner V, Lee HK, Lemieux H, Lerfall J, Lucchinetti E, Makrecka-
18 Kuka M, Meszaros AT, Moiso N, Molina AJA, Montaigne D, Moore AL, Murray AJ,
19 Nozickova K, Oliveira PF, Oliveira PJ, Orynbayeva Z, Palmeira CM, Patel HH, Pesta D, Petit
20 PX, Pichaud N, Pirkmajer S, Porter RK, Pranger F, Prochownik EV, Reboredo P, Renner-
21 Sattler K, Rohlena J, Røslund GV, Rossiter HB, Salvadego D, Scatena R, Schartner M,
22 Scheibye-Knudsen M, Schilling JM, Schlattner U, Schoenfeld P, Scott GR, Singer D, Sobotka
23 O, Spinazzi M, Stocker R, Sumbalova Z, Suravajhala P, Tanaka M, Tandler B, Tepp K,
24 Towheed A, Trivigno C, Tronstad KJ, Tyrrell DJ, Velika B, Vendelin M, Vercesi AE, Ward
25 ML, Watala C, Wei YH, Wieckowski MR, Wolff J, Wuest RCI, Zaugg M, Zorzano A

26

27 Supporting co-authors:

28 Arandarčikaitė O, Bakker BM, Batista Ferreira J, Bernardi P, Boetker HE, Borsheim E,
29 Borutaitė V, Bouitbir J, Calabria E, Calbet JA, Carvalho E, Chaurasia B, Clementi E, Collin
30 A, Das AM, De Palma C, Distefano G, Dubouchaud H, Duchon MR, Durham WJ, Dyrstad
31 SE, Fornaro M, Gan Z, Garlid KD, Garten A, Gourlay CW, Granata C, Haas CB, Haendeler J,
32 Hand SC, Hepple RT, Hickey AJ, Hoel F, Kainulainen H, Keppner G, Khamoui AV,
33 Klingenspor M, Koopman WJH, Kowaltowski AJ, Krajcova A, Lenaz G, MacMillan-Crow
34 LA, Malik A, Markova M, Mazat JP, Menze MA, Methner A, Muntané J, Muntean DM,
35 Neuzil J, Newsom S, O'Gorman D, Oliveira MT, Pak YMK, Pettersen IKN, Pulinilkunnil T,
36 Robinson MM, Ropelle ER, Salin K, Sandi C, Sazanov LA, Siewiera K, Silber AM, Skolik R,
37 Smenes BT, Soares FAA, Sokolova I, Sonkar VK, Stankova P, Swerdlow RH, Szabo I,
38 Thyfault JP, Tretter L, Vieyra A, Votion DM, Williams C, Zaugg K

39

40 **Updates:**

41 http://www.mitoeagle.org/index.php/MitoEAGLE_preprint_2017-09-21

42

Correspondence: Gnaiger E

Department of Visceral, Transplant and Thoracic Surgery, D. Swarovski Research Laboratory, Medical University of Innsbruck, Innrain 66/4, A-6020 Innsbruck, Austria

Email: erich.gnaiger@i-med.ac.at

Tel: +43 512 566796, Fax: +43 512 566796 20

43
44
45
46
47
48

49 This manuscript on 'The protonmotive force
50 and respiratory control' is a position
51 statement in the frame of COST Action
52 CA15203 MitoEAGLE. The list of co-authors
53 evolved from MitoEAGLE Working Group
54 Meetings and a **bottom-up** spirit of COST:
55 This is an open invitation to scientists and
56 students to join as co-authors, to provide a
57 balanced view on mitochondrial respiratory
58 control, a fundamental introductory
59 presentation of the concept of the
60 protonmotive force, and a critical discussion
61 on reporting data of mitochondrial
62 respiration in terms of metabolic flows and
63 fluxes. We plan a series of follow-up reports by the expanding MitoEAGLE Network, to increase
64 the scope of consensus-oriented recommendations and facilitate global communication and
65 collaboration.



66 We continue to invite comments and suggestions on the MitoEAGLE preprint (phase 2;
67 until **October 12**), particularly if you are an **early career investigator adding an open future-**
68 **oriented perspective**, or an **established scientist providing a balanced historical basis**. Your
69 critical input into the quality of the manuscript will be most welcome, improving our aims to be
70 educational, general, consensus-oriented, and practically helpful for students working in
71 mitochondrial respiratory physiology.

72 Please feel free to focus on a particular section in terms of direct input and references,
73 while evaluating the entire scope of the manuscript from the perspective of your expertise.

74 Your comments will be largely posted on the discussion page of the MitoEAGLE preprint
75 website. If you prefer to submit comments in the format of a referee's evaluation rather than a
76 contribution as a co-author, I will be glad to distribute your views to the updated list of co-
77 authors for a balanced response. We would ask for your consent on this open bottom-up policy.

78 We organize a MitoEAGLE session linked to our series of reports at the MiPconference
79 Nov 2017 in Hradec Kralove in close association with the MiPsociety (where you hopefully will
80 attend) and at EBEC 2018 in Budapest.

81 » http://www.mitoeagle.org/index.php/MiP2017_Hradec_Kralove_CZ

82

83 I thank you in advance for your feedback.

84 With best wishes,

85

86 Erich Gnaiger

87 Chair Mitochondrial Physiology Society - <http://www.mitophysiology.org>

88 Chair COST Action MitoEAGLE - <http://www.mitoeagle.org>

89 Medical University of Innsbruck, Austria

90

91	Contents
92	1. Introduction
93	2. Respiratory coupling states in mitochondrial preparations
94	2.1. <i>Definitions</i>
95	Mitochondrial preparations
96	Control and regulation
97	Respiratory control and response
98	Coupling control states
99	Pathway control states
100	The steady-state
101	2.2. <i>Three coupling states of mitochondrial preparations and residual oxygen consumption</i>
102	Coupling states and kinetic control
103	Phosphorylation, »P
104	LEAK, OXPHOS, ETS, ROX
105	2.3. <i>Classical terminology for isolated mitochondria</i>
106	States 1-5
107	2.4. <i>Coupling states and respiratory rates</i>
108	3. States and rates
109	3.1. <i>The protonmotive force and proton flow</i>
110	Faraday constant
111	Electrical part of the protonmotive force
112	Chemical part of the protonmotive force
113	3.2. <i>Forces and flows in physics and irreversible thermodynamics</i>
114	Vectorial and scalar forces, and fluxes
115	Coupling
116	Coupled versus bound processes
117	4. Normalization: flows and fluxes
118	4.1. <i>Flux per chamber volume</i>
119	4.2. <i>Extensive expressions and size-specific normalization</i>
120	Extensive quantities
121	Size-specific quantities
122	Molar quantities
123	Flow per system, I
124	Size-specific flux, J
125	Sample concentration, C_{mX}
126	Mass-specific flux, J_{mX,O_2}
127	Number concentration, C_{NX}
128	Flow per sample entity, I_{X,O_2}
129	4.2. <i>Normalization for mitochondrial content</i>
130	Mitochondrial concentration, C_{mte} , and mitochondrial markers
131	Mitochondria-specific flux, J_{mte,O_2}
132	4.3. <i>Conversion: oxygen, protons, ATP</i>
133	5. Conclusions
134	6. References
135	

136 **Abstract**

137 Clarity of concepts and consistency of nomenclature are trademarks of a research field across
138 its specializations, facilitating transdisciplinary communication and education. As research and
139 knowledge of mitochondrial physiology expand, the necessity for harmonizing nomenclature
140 concerning mitochondrial respiratory states and rates has become apparent. Peter Mitchell's
141 concept of the protonmotive force establishes the links between electrical and chemical
142 components of energy transformation and coupling in oxidative phosphorylation. This unifying
143 concept provides the framework for developing a consistent terminology of mitochondrial
144 physiology and bioenergetics. We follow IUPAC guidelines on general terms of physical
145 chemistry, extended by concepts of open systems and irreversible thermodynamics. We align
146 the nomenclature of classical bioenergetics on respiratory states with a concept-driven
147 constructive terminology to address the meaning of each respiratory state. Standards for
148 evaluation of respiratory states must be followed for the development of databases of
149 mitochondrial respiratory function in species, tissues and cells studied under diverse
150 physiological and experimental conditions.

151

152 *Keywords:* Mitochondrial respiratory control, coupling control, mitochondrial
153 preparations, protonmotive force, chemiosmotic theory, oxidative phosphorylation, OXPHOS,
154 efficiency, electron transfer system, ETS; proton leak, LEAK, residual oxygen consumption,
155 ROX, State 2, State 3, State 4, normalization, flow, flux

156

157

158

159 **Box 1:**
160 **In brief -**
161 **mitochondria**
162 **and Bioblasts**

- * Does the public expect biologists to understand Darwin's theory of evolution?
- * Do students expect that researchers of bioenergetics can explain Mitchell's theory of chemiosmotic energy transformation?

163 **Mitochondria** are dynamic organelles contained within eukaryotic cells, with a double
164 membrane. The inner mitochondrial membrane shows dynamic tubular and disk-shaped cristae
165 that separate the mitochondrial matrix, *i.e.* the internal mitochondrial compartment, and the
166 intermembrane space; the latter being enclosed by the outer mitochondrial membrane.
167 Mitochondria were described for the first time in 1857 by Rudolph Albert von Kölliker as
168 granular structures or 'sarkosomes'. In 1886 Richard Altmann called them 'bioblasts' (published
169 1894). The word 'mitochondrium' (Greek mitos: thread; chondros: granule) was introduced by
170 Carl Benda (1898). Mitochondria are the oxygen consuming electrochemical generators which
171 evolved from endosymbiotic bacteria (Margulis 1970). The bioblasts of Richard Altmann
172 (1894) include not only the mitochondria as presently defined, but also symbiotic and free-
173 living bacteria. Mitochondria are the structural and functional elemental units of cell respiration,
174 where cell respiration is defined as the consumption of oxygen coupled to electrochemical
175 proton translocation across the inner mitochondrial membrane. In the process of oxidative
176 phosphorylation (OXPHOS), the reduction of O₂ is electrochemically coupled to conservation
177 of energy in the form of ATP (Mitchell 2011). As part of the OXPHOS system, these
178 powerhouses of the cell contain the transmembrane respiratory complexes (*i.e.* FMN, Fe-S and
179 cytochrome *b*, *c*, *aa*₃ redox systems), alternative dehydrogenases and oxidases, the coenzyme
180 ubiquinone (Coenzyme Q, CoQ) and ATP synthase together with the enzymes of the
181 tricarboxylic acid cycle and the fatty acid oxidation enzymes, ion transporters, including
182 substrate, co-factor and metabolite transporters as well as proton pumps, and mitochondrial
183 kinases related to energy transfer pathways. The mitochondrial proteome comprises over 1,200
184 proteins (Mitochondria), mostly encoded by nuclear DNA (nDNA), with a variety of functions,

185 many of which are relatively well known (*e.g.* apoptosis-regulating proteins), are still under
186 investigation, or need to be identified (alanine transporter). Mitochondria maintain several
187 copies of their own genome (hundred to thousands per cell) which is maternally inherited and
188 known as mitochondrial DNA (mtDNA). mtDNA is 16.5 Kb in length, contains 13 protein-
189 coding genes for subunits of the transmembrane respiratory Complexes CI, CIII, CIV and ATP
190 synthase, and also encodes 22 tRNAs and the mitochondrial 16S and 12S rRNA. The
191 mitochondrial genome is both regulated and supplemented by nuclear-encoded mitochondrial
192 targeted proteins. Evidence has accumulated that additional gene content is encoded in the
193 mitochondrial genome, *e.g.* microRNAs, smithRNAs, and even additional proteins. The inner
194 mitochondrial membrane contains the non-bilayer phospholipid cardiolipin, which is not
195 present in any other eukaryotic cellular membrane. Cardiolipin promotes the formation of
196 respiratory supercomplexes, which are supramolecular assemblies based upon specific, though
197 dynamic, interactions between individual respiratory complexes (Lenaz *et al.* 2017). There is a
198 constant crosstalk between mitochondria and the other cellular components at the
199 transcriptional or post-translational level, and through cell signalling in response to varying
200 energy demands (Quiros *et al.* 2016). Mitochondrial morphology can change in response to
201 energy requirements of the cell via processes known as fusion and fission through which
202 mitochondria can communicate within a network, and in various pathological states which
203 cause swelling or dysregulation of fission and fusion. Mitochondrial dysfunction is associated
204 with a wide variety of genetic and degenerative diseases. Therefore, a better understanding of
205 mitochondrial physiology will improve our understanding of the etiology of disease and the
206 diagnostic repertoire of mitochondrial medicine. Abbreviation: mt, as generally used in
207 mtDNA. Mitochondrion is singular and mitochondria is plural.

208 *‘For the physiologist, mitochondria afforded the first opportunity for an experimental*
209 *approach to structure-function relationships, in particular those involved in active transport,*

210 *vectorial metabolism, and metabolic control mechanisms on a subcellular level* (Ernster and
211 Schatz 1981).

212

213 **1. Introduction**

214 Mitochondria are the powerhouses of the cell with numerous physiological, molecular,
215 and genetic functions (**Box 1**). Every study of mitochondrial function and disease is faced with
216 **E**volution, **A**ge, **G**ender and sex, **L**ifestyle, and **E**nvironment (EAGLE) as essential background
217 conditions characterizing the individual patient or subject, cohort, species, tissue and to some
218 extent even cell line. As a large and highly coordinated group of laboratories and researchers,
219 the global MitoEAGLE Network's mission is to generate the necessary scale, type, and quality
220 of consistent data sets and conditions to address this intrinsic complexity. Harmonization of
221 experimental protocols and implementation of a quality control and data management system
222 is required to interrelate results gathered across a spectrum of studies and to generate a
223 rigorously monitored database focused on mitochondrial respiratory function. In this way,
224 researchers within the same and across different disciplines will be positioned to compare their
225 findings to an agreed upon set of clearly defined and accepted international standards.

226 Reliability and comparability of quantitative results depend on the accuracy of
227 measurements under strictly-defined conditions. A conceptually clearly-defined framework is
228 also required to warrant meaningful interpretation and comparability of experimental outcomes
229 carried out by research groups at different institutes. With an emphasis on quality of research,
230 collected data can be useful far beyond the specific question of a specific experiment. Vague or
231 ambiguous jargon can lead to confusion and may relegate valuable signals to wasteful noise.
232 For this reason, measured values must be expressed in standardized units for each parameter
233 used to define mitochondrial respiratory function. Standardization of nomenclature and
234 technical terms is essential to improve the awareness of the intricate meaning of divergent
235 scientific vocabulary. The focus on coupling states in mitochondrial preparations is a first step

236 in the attempt to generate a harmonized and conceptually oriented nomenclature in
237 bioenergetics and mitochondrial physiology. Coupling states of intact cells and respiratory
238 control by fuel substrates and specific inhibitors of respiratory enzymes will be reviewed in
239 subsequent communications.

240

241 **2. Respiratory coupling states in mitochondrial preparations**

242 *‘Every professional group develops its own technical jargon for talking about*
243 *matters of critical concern ... People who know a word can share that idea with*
244 *other members of their group, and a shared vocabulary is part of the glue that holds*
245 *people together and allows them to create a shared culture’ (Miller 1991).*

246

247 *2.1. Definitions*

248 **Mitochondrial preparations** are defined as either isolated mitochondria, or tissue and
249 cellular preparations in which the barrier function of the plasma membrane is disrupted. The
250 plasma membrane separates the cytosol, nucleus and organelles (the intracellular compartment)
251 from the environment of the cell. The plasma membrane consists of a lipid bilayer, embedded
252 proteins and attached organic molecules which collectively control the selective permeability
253 of ions, organic molecules and particles across the cell boundary. The intact plasma membrane,
254 therefore, prevents the passage of many water-soluble mitochondrial substrates, such as
255 succinate or ADP, that are required for the analysis of respiratory capacity at kinetically
256 saturating concentrations, thus limiting the scope of investigations into mitochondrial
257 respiratory function in intact cells. The cholesterol content of the plasma membrane is high
258 compared to mitochondrial membranes. Therefore, mild detergents, such as digitonin and
259 saponin, can be applied to selectively permeabilize the plasma membrane by interaction with
260 cholesterol and allow free exchange of cytosolic components with ions and organic molecules
261 of the immediate cell environment, while maintaining the integrity and localization of

262 organelles, cytoskeleton and the nucleus. Application of optimum concentrations of these mild
263 detergents leads to the complete loss of cell viability, tested by nuclear staining, while
264 mitochondrial function remains unaffected, as shown by the lack of a respiratory response of
265 respiration of isolated mitochondria to the addition of such low concentrations of digitonin and
266 saponin. Mechanical or chemical permeabilization is applied in tissue homogenates containing
267 all components of the cell in the crude homogenate at highly diluted concentrations. Likewise,
268 in permeabilized tissues or cells the functional and structural integrity of mitochondria are
269 largely maintained. All mitochondria are retained in chemically permeabilized mitochondrial
270 preparations and crude tissue homogenates. In the preparation of isolated mitochondria the cells
271 or tissues are homogenized, and the mitochondria are separated from other cell fractions and
272 purified by centrifugation, entailing the loss of a significant fraction of mitochondria. The term
273 mitochondrial preparation does not include further fractionation of mitochondrial components,
274 as well as submitochondrial particles.

275 **Control and regulation:** The terms metabolic *control* and *regulation* are frequently used
276 synonymously, but are distinguished in metabolic control analysis: ‘We could understand the
277 regulation as the mechanism that occurs when a system maintains some variable constant over
278 time, in spite of fluctuations in external conditions (homeostasis of the internal state). On the
279 other hand, metabolic control is the power to change the state of the metabolism in response to
280 an external signal’ (Fell 1997). Respiratory control may be induced by experimental control
281 signals that *exert* an influence on: (1) ATP demand and ADP phosphorylation rate; (2) fuel
282 substrate, pathway competition and oxygen availability, *e.g.*, starvation and hypoxia; (3) the
283 protonmotive force, redox states, flux-force relationships, coupling and efficiency; (4) Ca^{2+} and
284 other ions including H^+ ; (5) inhibitors, *e.g.*, nitric oxide or intermediary metabolites, such as
285 oxaloacetate. *Mechanisms* of respiratory control and regulation include adjustments of (1)
286 enzyme activities by allosteric mechanisms and phosphorylation, (2) enzyme content,
287 concentrations of cofactors and conserved moieties (such as adenylates, nicotinamide adenine

288 dinucleotide [NAD⁺/NADH], coenzyme Q, cytochrome *c*); (3) metabolic channeling by
289 supercomplexes; and (4) mitochondrial density (enzyme concentrations and membrane area)
290 and morphology (cristae folding, fission and fusion). (5) Mitochondria are targeted directly by
291 hormones, thereby affecting their energy metabolism (Lee *et al.* 2013; Gerö and Szabo 2016;
292 Price and Dai 2016; Moreno *et al.* 2017). Evolutionary or acquired differences in the genetic
293 and epigenetic basis of mitochondrial function (or dysfunction) between subjects and gene
294 therapy; age; gender, biological sex, and hormone concentrations; life style including exercise
295 and nutrition; and environmental issues including thermal, atmospheric, toxicological and
296 pharmacological factors, exert an influence on all control mechanisms listed above (for reviews,
297 see Brown 1992; Gnaiger 1993a, 2009; 2014; Paradies *et al.* 2014; Morrow *et al.* 2017).

298 **Respiratory control and response:** There is a difference between control by a fixed
299 component of a metabolic system or module, e.g. ATP synthase, and the response to an
300 experimental variable, *e.g.*, fuel substrate or ADP. Whilst lack of control by a metabolic
301 module, *e.g.* phosphorylation system, does mean that there will be no response to a variable
302 activating it, *e.g.* [ADP], the reverse is not true; *i.e.*, lack of response to [ADP] does not exclude
303 the phosphorylation system from having some degree of control. The degree of control of a
304 component of the OXPHOS system on an output variable of the system, such as oxygen flux,
305 will in general be different from the degree of control on other outputs, such as phosphorylation
306 flux, cytochrome redox states, protonmotive force, phosphorylation potential, and proton leak
307 flux (**Table 1**). As such, it is necessary to be specific as to which output is under consideration.
308 Respiratory control is insufficiently specific in the context of specific interpretations (Fell
309 1997).

310 **Respiratory coupling control:** Respiratory control is monitored in a mitochondrial
311 preparation under conditions defined as respiratory states. When phosphorylation of ADP to
312 ATP is stimulated or depressed, an increase or decrease is observed in electron flow linked to
313 oxygen consumption in ‘controlled’ coupling states in intact mitochondria. Alternatively,

314 coupling of electron transfer with phosphorylation is disengaged by disruption of the integrity
315 of the inner mitochondrial membrane or by uncouplers, functioning like a clutch in a
316 mechanical system. The corresponding coupling control state is characterized by high levels of
317 oxygen consumption without control by phosphorylation ('uncontrolled state'; classical
318 terminology). Energetic coupling is defined in **Box 2**. Respiratory control refers to the ability
319 of mitochondria to adjust oxygen consumption in response to external control signals by
320 engaging various mechanisms of control and regulation. Loss of coupling by intrinsic
321 uncoupling and decoupling, or pathological dyscoupling lowers the efficiency. Such
322 generalized uncoupling is different from switching to mitochondrial pathways that involve
323 fewer than three proton pumps ('coupling sites': Complexes CI, CIII and CIV), bypassing CI
324 through multiple electron entries into the Q-junction (**Fig. 1**). A bypass of CIII and CIV is
325 provided by alternative oxidases, which reduce oxygen without proton translocation.
326 Reprogramming of mitochondrial pathways may be considered as a switch of gears (changing
327 the stoichiometry) rather than uncoupling (loosening the stoichiometry).

328 **Pathway control states** are obtained in mitochondrial preparations by depletion of
329 endogenous substrates and addition to the mitochondrial respiration medium of fuel substrates
330 (CHNO) and specific inhibitors, activating selected mitochondrial pathways (**Fig. 1**). Coupling
331 control states and pathway control states are complementary, since mitochondrial preparations
332 depend on an exogenous supply of pathway-specific fuel substrates and oxygen (Gnaiger 2014).

333

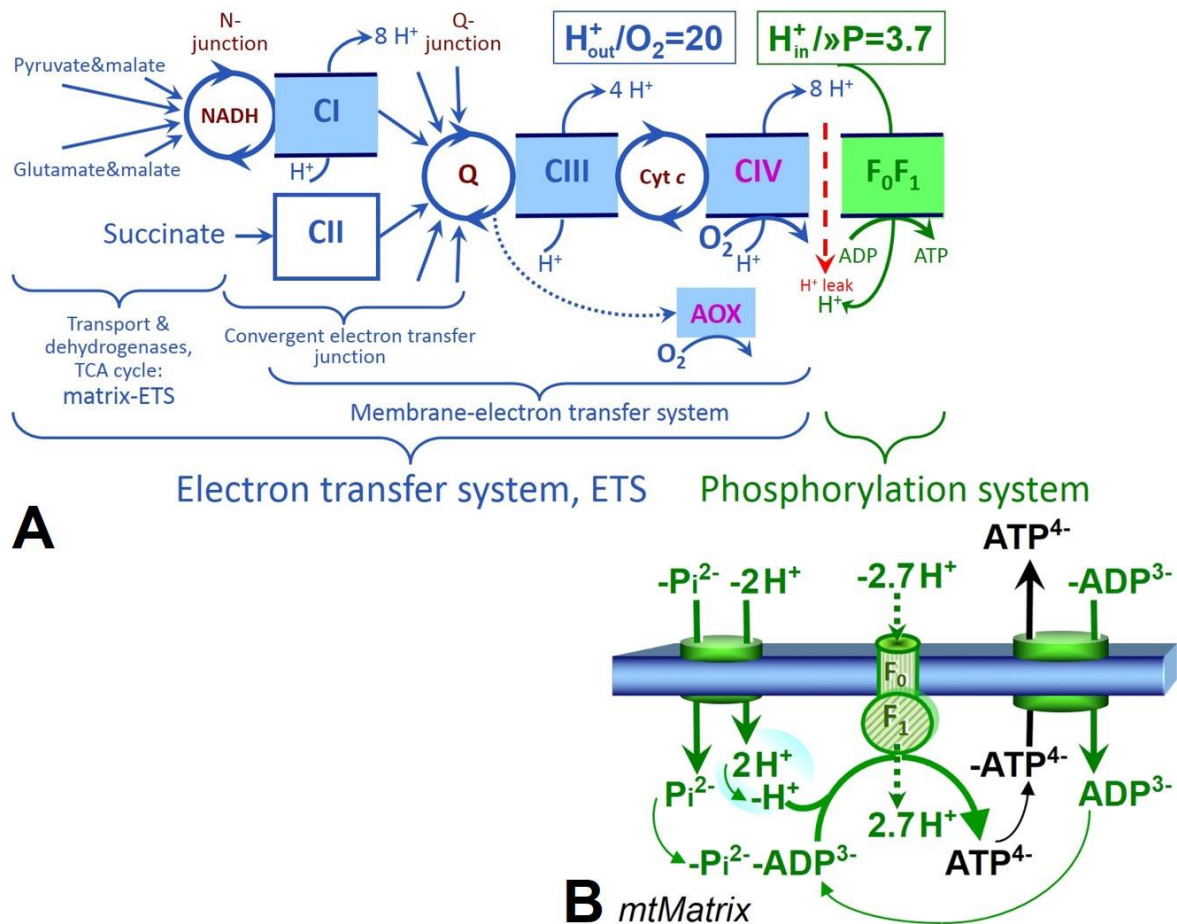
334 *2.2. Three coupling states of mitochondrial preparations and residual oxygen consumption*

335 **Coupling control states:** To extend the classical nomenclature on mitochondrial
336 coupling states (Section 2.3) by a concept-driven terminology that incorporates explicit
337 information on the nature of the respiratory states, the terminology must be general and not
338 restricted to any particular experimental protocol or mitochondrial preparation (Gnaiger 2009).
339 We focus primarily on the conceptual 'why', along with clarification of the experimental 'how'.

340 In the following section, the concept-driven terminology is explained and coupling states are
341 defined. The capacity of *oxidative phosphorylation*, OXPHOS, provides diagnostic reference
342 values for physiological respiratory capacities of defined pathways of core energy metabolism
343 and is, therefore, measured at kinetically saturating concentrations of ADP and inorganic
344 phosphate, P_i . The *oxidative* capacity of the electron transfer system, ETS, reveals the limitation
345 of OXPHOS capacity mediated by the *phosphorylation* system. ETS capacity is measured as
346 noncoupled respiration by application of *external uncouplers*. The contribution of *intrinsically*
347 *uncoupled* oxygen consumption is most easily studied by not stimulating or arresting
348 phosphorylation, when oxygen consumption compensates mainly for the proton leak; the
349 corresponding states are collectively classified as LEAK states (**Table 1**). Coupling states of
350 mitochondrial preparations can be compared in any defined mitochondrial pathway control state
351 (**Fig. 1**). Fuel substrates and ETS inhibitors are kept constant while (1) adding ADP or P_i , (2)
352 inhibiting the phosphorylation system, and (3) performing uncoupler titrations.

353 **Respiratory capacities and kinetic control:** Coupling control states are established in
354 the study of mitochondrial preparations to obtain reference values for various output variables.
355 Physiological conditions *in vivo* may deviate substantially from these experimentally obtained
356 states. Since kinetically saturating concentrations, *e.g.* of ADP or oxygen, may not apply to
357 physiological intracellular conditions, relevant information is obtained in studies of kinetic
358 responses to conditions intermediate between the LEAK state at zero [ADP] and the OXPHOS
359 state at saturating [ADP], or of respiratory capacities in the range between kinetically saturating
360 $[O_2]$ and anoxia (Gnaiger 2001). We define respiratory capacities, comparable to channel
361 capacity in information theory, as the upper bound of the rate of respiration measured in defined
362 coupling and pathway control states of mitochondrial preparations (**Box 3**).

363



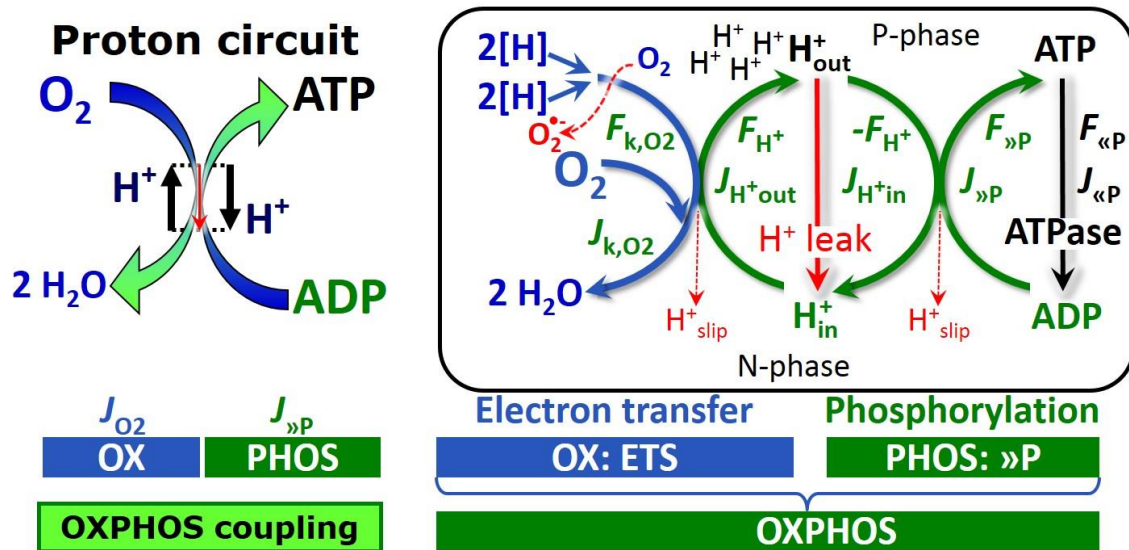
364

365 **Fig. 1. The mitochondrial respiratory system and oxidative phosphorylation. (A)** The electron
 366 transfer system, ETS, and coupling to the phosphorylation system. Multiple convergent electron transfer
 367 pathways are shown from NADH and succinate; additional arrows indicate electron entry through
 368 electron transferring flavoprotein, glycerophosphate dehydrogenase, dihydro-oroate dehydrogenase,
 369 choline dehydrogenase, and sulfide-ubiquinone oxidoreductase. The branched pathway of oxygen
 370 consumption by alternative quinol oxidase (AOX) is indicated by the dotted arrow. H_{out}^+ / O_2 is the ratio of
 371 outward proton flux from the matrix space to catabolic O_2 flux in the NADH-linked pathway. $H_{in}^+ / \gg P$ is
 372 the ratio of inward proton flux from the inter-membrane space to the endergonic flux of phosphorylation
 373 of ADP to ATP. Due to proton leak and slip these are not fixed stoichiometries. (B) Phosphorylation
 374 system consisting of the F_1F_0 ATP synthase, adenine nucleotide translocase, and the inorganic
 375 phosphate transporter. The $H_{in}^+ / \gg P$ stoichiometry is the sum of the coupling stoichiometry in the ATP
 376 synthase reaction ($-2.7 H^+$ from the intermembrane space, $2.7 H^+$ to the matrix) and the proton balance
 377 in the translocation of ADP^{2-} , ATP^{3-} and P_i^{2-} . See Eqs. 11 and 12 for further explanation. Modified from
 378 (A) Lemieux *et al.* (2017) and (B) Gnaiger (2014).

379

380 **Phosphorylation, »P:** *Phosphorylation* in the context of OXPHOS is defined as
381 phosphorylation of ADP to ATP. On the other hand, the term phosphorylation is used generally
382 in many different contexts, *e.g.* protein phosphorylation. This justifies consideration of a
383 symbol more discriminating and specific than P as used in the P/O ratio (phosphate to atomic
384 oxygen ratio), where P indicates phosphorylation of ADP to ATP or GDP to GTP. We propose
385 the symbol »P for the endergonic direction of phosphorylation ADP→ATP, and likewise the
386 symbol «P for the corresponding exergonic hydrolysis ATP→ADP (**Fig. 2**). ##ATP synthase
387 is the proton pump of the phosphorylation system (**Fig. 1B**). »P may also involve substrate-
388 level phosphorylation as part of the tricarboxylic acid cycle (succinyl-CoA ligase) and
389 phosphorylation of ADP catalyzed by phosphoenolpyruvate carboxykinase, adenylate kinase,
390 creatine kinase, hexokinase and nucleoside diphosphate kinase (NDPK). Kinase cycles are
391 involved in intracellular energy transfer and signal transduction for regulation of energy flux.
392 In isolated mammalian mitochondria ATP production catalyzed by adenylate kinase, $2\text{ADP} \leftrightarrow$
393 $\text{ATP} + \text{AMP}$, proceeds without fuel substrates in the presence of ADP (Komlódi and Tretter
394 2017). $J_{\text{»P}}/J_{\text{O}_2}$ (»P/O₂) is two times the ‘P/O’ ratio of classical bioenergetics. The effective
395 »P/O₂ ratio is diminished by: (1) the proton leak across the inner mitochondrial membrane from
396 low pH in the P-phase to high pH in the N-phase (P, positive; N, negative); (2) cycling of other
397 cations; (3) proton slip in the proton pumps when a proton effectively is not pumped; and (4)
398 electron leak in the univalent reduction of oxygen (O₂; dioxygen) to superoxide anion radical
399 (O₂^{•-}).

400



401

402 **Fig. 2. The proton circuit and coupling in oxidative phosphorylation (OXPHOS).** Oxygen flux, J_{k,O_2} ,
 403 in a catabolic reaction k is coupled to the phosphorylation of ADP to ATP, $J_{»P}$, by the proton pumps of
 404 the electron transfer system, ETS, pushing the outward proton flux, J_{H^+out} , and generating the output
 405 protonmotive force, $F_{H^+} \equiv F_{H^+out}$. ATP synthase is coupled to inward proton flux, J_{H^+in} , to phosphorylate
 406 ADP to ATP, driven by the input protonmotive force, $F_{H^+in} = -F_{H^+}$. $2[H]$ indicates the reduced hydrogen
 407 equivalents of fuel substrates that provide the chemical input force, F_{k,O_2} [kJ/mol O_2], of the catabolic
 408 reaction k with oxygen (Gibbs energy of reaction per mole O_2 consumed in reaction k), typically in the
 409 range of -460 to -480 kJ/mol. The output force is given by the phosphorylation potential difference (ADP
 410 phosphorylated to ATP), $F_{»P}$, which varies *in vivo* ranging from about 48 to 62 kJ/mol under physiological
 411 conditions. Fluxes, J_B , and forces, F_B , are expressed in either chemical units, [$mol \cdot s^{-1} \cdot L^{-1}$] and [$J \cdot mol^{-1}$]
 412 respectively, or electrical units, [$C \cdot s^{-1} \cdot L^{-1}$] and [$J \cdot C^{-1}$] respectively, per volume, V [L], of the system
 413 (defined by the system boundaries shown as the black line). Modified from Gnaiger (2014).

414

415 **Box 2: Coupling, power and efficiency, at constant temperature and pressure**

416 Energetic coupling means that two processes of energy transformation are linked such that the
 417 input power, P_{in} , is the driving element of the output power, P_{out} , and the out/input power ratio
 418 is the efficiency. In general, power is work per unit time [$J \cdot s^{-1} = W$]. When describing a system
 419 with volume V without information on the internal structure, the output is defined as the *external*
 420 work (exergy) performed by the *total* system on its environment. Such as system may be open

421 for any type of exchange, or closed and thus allowing only heat and work to be exchanged
 422 across the system boundaries. This is the classical black box approach of thermodynamics. In
 423 contrast, in a colourful compartmental analysis of *internal* energy transformations (**Fig. 2**), the
 424 system is structured and described by definition of internal compartments (with information on
 425 the heterogeneity of the system) and analysis of separate parts, *i.e.* a sequence of *partial* energy
 426 transformations, tr. In general, power per unit volume, P_{tr}/V [W.L⁻¹], is the product of a volume-
 427 specific flux, J_{tr} , and its conjugated force, F_{tr} , and is closely linked to the dissipation function
 428 using the terminology of irreversible thermodynamics (Prigogine 1967; Gnaiger 1993a,b). In
 429 **Fig. 2**, the scalar catabolic reaction of oxygen consumption is expressed as oxygen flux per
 430 volume, J_{k,O_2} . It is coupled to vectorial translocation of protons across the inner mitochondrial
 431 membrane, from the negative compartment (matrix) to the positive compartment (inter-
 432 membrane space). Compartmental vectorial translocation does not, however, implicate a vector
 433 force or gradient across the membrane with defined spatial direction, but the protonmotive force
 434 is defined merely as an electrochemical potential difference between two compartments. Output
 435 power of proton translocation and catabolic input power are (**Fig. 2**),

436 Output:
$$P_{H^+out}/V = J_{H^+out} \cdot F_{H^+}$$

437 Input:
$$P_k/V = J_{k,O_2} \cdot F_{k,O_2}$$

438 F_{k,O_2} is the exergonic input force with a negative sign, and, F_{H^+} , is the endergonic output force
 439 with a positive sign (**Box 4**). Ergodynamic efficiency is the ratio of output/input power, or the
 440 flux ratio times force ratio (Gnaiger 1993a,b),

441
$$\varepsilon = \frac{P_{H^+out}}{-P_k} = \frac{J_{H^+out}}{J_{k,O_2}} \cdot \frac{F_{H^+}}{-F_{k,O_2}}$$

442 The concept of incomplete coupling relates exclusively to the first term, *i.e.* the flux ratio, or
 443 H^+_{out}/O_2 ratio (**Fig. 1**). Likewise, respirometric definitions of the »P/O₂ ratio and biochemical
 444 coupling efficiency (Section 3.2) consider flux ratios. In a completely coupled process, the
 445 power efficiency, ε , depends entirely on the force ratio, ranging from zero efficiency at an

446 output force of zero, to the limiting output force and maximum efficiency of 1.0, when the total
447 power of the coupled process, $P_t = P_k + P_{H+out}$, equals zero, and any net flows are zero at
448 ergodynamic equilibrium of a coupled process. Thermodynamic equilibrium is defined as the
449 state when all potentials (all forces) are dissipated and equilibrate towards their minima of zero.
450 In a fully or completely coupled process, output and input fluxes are directly proportional in a
451 fixed ratio technically defined as a stoichiometric relationship (a gear ratio in a mechanical
452 system). Such maximal stoichiometric output/input flux ratios are considered in OXPHOS
453 analysis as the upper limits or mechanistic H^+_{out}/O_2 and $\gg P/O_2$ ratios (**Fig. 1**).

454

455

456 **Box 3: Mitochondrial and cell respiration**

457 Mitochondrial and cell respiration is the process of highly exothermic energy transformation in
458 which scalar redox reactions are coupled to vectorial ion translocation across a semipermeable
459 membrane, which separates the small volume of a bacterial cell or mitochondrion from the
460 larger volume of its surroundings. The electrochemical exergy can be partially conserved in the
461 phosphorylation of ADP to ATP or in ion pumping, or dissipated in an electrochemical short-
462 circuit. Respiration is thus clearly distinguished from fermentation as the counterpart of core
463 energy metabolism. Respiration is separated in mitochondrial preparations from the partial
464 contribution of fermentative pathways of the intact cell. According to this definition, residual
465 oxygen consumption, as measured after inhibition of the mitochondrial electron transfer system,
466 is to be subtracted from total oxygen consumption to obtain baseline corrected (bc) respiration.

467

468 **The steady-state:** Mitochondria represent a thermodynamically open system functioning
469 as a biochemical transformation system in non-equilibrium states. State variables (protonmotive
470 force; redox states) and metabolic fluxes (*rates*) are measured in defined mitochondrial
471 respiratory *states*. Strictly, steady states can be obtained only in open systems, in which changes

472 due to *internal* transformations, e.g., O₂ consumption, are instantaneously compensated for by
 473 *external* flows e.g., O₂ supply, such that oxygen concentration does not change in the system
 474 (Gnaiger 1993b). Mitochondrial respiratory states monitored in closed systems satisfy the
 475 criteria of pseudo-steady states for limited periods of time, when changes in the system
 476 (concentrations of O₂, fuel substrates, ADP, P_i, H⁺) do not exert significant effects on metabolic
 477 fluxes (respiration, phosphorylation). Such pseudo-steady states require respiratory media with
 478 sufficient buffering capacity and kinetically saturating concentrations of substrates to be
 479 maintained, and thus depend on the kinetics of the processes under investigation. Proton
 480 turnover, $J_{\infty H^+}$, and ATP turnover, $J_{\infty P}$, proceed in the steady-state at constant F_{H^+} , when $J_{\infty H^+} =$
 481 $J_{H^+out} = J_{H^+in}$, and at constant $F_{\gg P}$, when $J_{\infty P} = J_{\gg P} = J_{\ll P}$ (**Fig. 2**).

482

483 **Table 1. Coupling states and residual oxygen consumption in mitochondrial**
 484 **preparations in relation to respiration and phosphorylation rate, J_{O_2} and $J_{\gg P}$, and**
 485 **protonmotive force, F_{H^+} .** Coupling states are established at kinetically saturating
 486 concentrations of fuel substrates and O₂.

State	J_{O_2}	$J_{\gg P}$	F_{H^+}	Inducing factors	Limiting factors
LEAK	L ; low proton leak- dependent respiration;	0	max.	Proton leak, slip, and cation cycling	$J_{\gg P}=0$: (1) without ADP, L_N ; (2) max. ATP/ADP ratio, L_T ; or (3) inhibition of the ADP phosphorylation system, L_{Omy}
OXPHOS	P ; high ADP- stimulated respiration	max.	high	Kinetically saturating [ADP] and [P _i]	$J_{\gg P}$ by phosphorylation system; or J_{O_2} by electron transfer system
ETS	E ; max. noncoupled respiration	0	low	Optimal external uncoupler concentration for maximum oxygen flux	J_{O_2} by electron transfer system
ROX	R_{ox} ; min. residual O ₂ consumption	0	0	Non-ETS oxidation reactions	Full inhibition of ETS or absence of substrates

487

514 *uncoupled* respiration, *e.g.*, as a consequence of opening the permeability transition pore.
515 Dyscoupled respiration is distinguished from the experimentally induced *noncoupled*
516 respiration in the ETS state. Under physiological conditions, the proton leak is the dominant
517 contributor to the overall leak current.

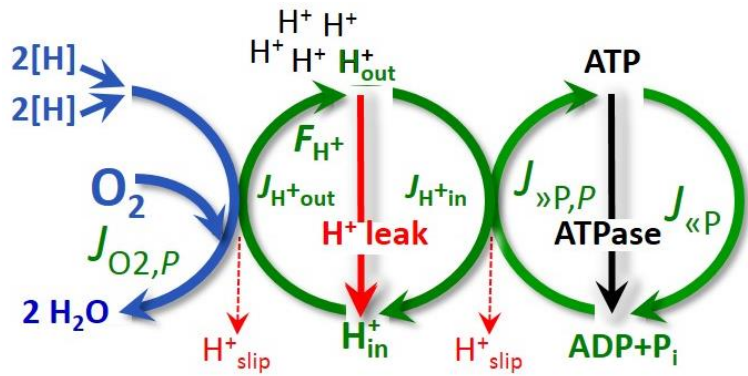
518 **Proton slip:** Proton slip is the *decoupled* process in which protons are only partially
519 translocated by a proton pump of the ETS and slip back to the original compartment (Dufour *et*
520 *al.* 1996). Proton slip can also happen in association with the ATP-synthase, in which case the
521 proton slips downhill across the membrane to the matrix without contributing to ATP synthesis.
522 In each case, proton slip is a property of the proton pump and increases with the turnover rate
523 of the pump.

524 **Cation cycling:** Proton leak is a leak current of protons. There can be other cation
525 contributors to leak current including calcium and probably magnesium. Calcium current is
526 balanced by mitochondrial Na/Ca exchange, which is balanced by Na/H exchange or K/H
527 exchange. This is another effective uncoupling mechanism different from proton leak and slip.

528 Small differences of terms, *e.g.*, uncoupled, noncoupled, are easily overlooked and may
529 be erroneously perceived as identical. Even with an attempt at rigorous definition, the common
530 use of such terms may remain vague (**Table 2**).

531 **OXPHOS state (Fig. 4):**

532 OXPHOS state is defined as the
 533 respiratory state with kinetically
 534 saturating concentrations of O_2 ,
 535 respiratory and phosphorylation
 536 substrates, and absence of
 537 exogenous uncoupler, which
 538 provides an estimate of the
 539 maximal capacity of OXPHOS in
 540 any given pathway control state.



541 **Fig. 4. OXPHOS state:** Phosphorylation, J_{P} , is stimulated
 542 by kinetically saturating [ADP] and inorganic phosphate, [Pi],
 543 and is supported by a high protonmotive force, F_{H^+} . O_2 flux,
 544 $J_{O_2,P}$, is highly coupled at a maximum $\gg P/O_2$ ratio, $J_{\gg P,P}/J_{O_2,P}$
 545 (See also Fig. 2).

541 Respiratory capacities at kinetically saturating substrate concentrations provide reference
 542 values or upper limits of performance, aiming at the generation of data sets for comparative
 543 purposes. Any effects of substrate kinetics are thus separated from reporting actual
 544 mitochondrial capacity for oxidation during coupled respiration, against which physiological
 545 activities can be evaluated.

546 As discussed previously, 0.2 mM ADP does not fully saturate flux in isolated
 547 mitochondria (Gnaiger 2001; Puchowicz *et al.* 2004); greater ADP concentration is required,
 548 particularly in permeabilized muscle fibres and cardiomyocytes, to overcome limitations by
 549 intracellular diffusion and by the reduced conductance of the outer mitochondrial membrane
 550 (Jepihhina *et al.* 2011, Illaste *et al.* 2012, Simson *et al.* 2016) either through interaction with
 551 tubulin (Rostovtseva *et al.* 2008) or other intracellular structures (Birkedal *et al.* 2014). In
 552 permeabilized muscle fibre bundles of high respiratory capacity, the apparent K_m for ADP
 553 increases up to 0.5 mM (Saks *et al.* 1998), indicating that >90% saturation is reached only at
 554 >5 mM ADP. Similar ADP concentrations are also required for accurate determination of
 555 OXPHOS capacity in human clinical cancer samples and permeabilized cells (ref).

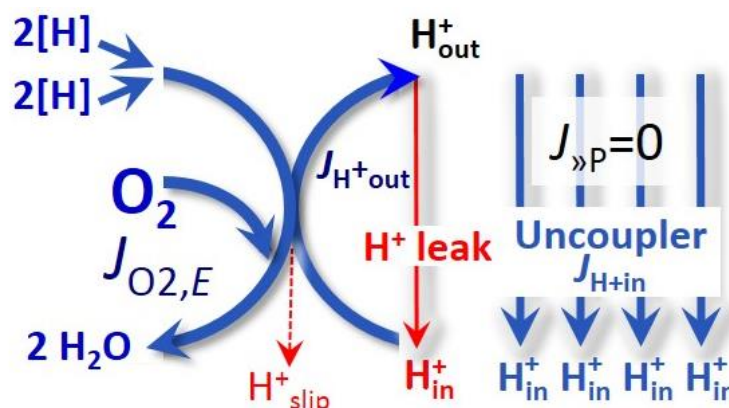
556

557 **Table 2. Distinction of terms related to coupling.**

Term	Respiration	$\gg P/O_2$	Note
Fully coupled	$P - L$	Max.	OXPHOS capacity corrected for LEAK respiration (Fig. 6)
Coupled	P	High	Phosphorylating respiration with a variable component of intrinsic LEAK respiration (Fig. 4)
Uncoupled, Decoupled	L	0	Non-phosphorylating respiration without added protonophore (Fig. 3)
Noncoupled	E	0	Non-phosphorylating respiration stimulated to maximum flux at optimum uncoupler concentration (Fig. 5)
Dyscoupled	P	Low	Pathologically increased uncoupling, mitochondrial dysfunction

558

559 **ETS state (Fig. 5):** The
 560 ETS state is defined as the
 561 *noncoupled* state with kinetically
 562 saturating concentrations of O_2 ,
 563 respiratory substrate and
 564 optimum *exogenous* uncoupler
 565 concentration for maximum O_2
 566 flux, as an estimate of oxidative
 567 ETS capacity. Inhibition of



568 **Fig. 5. ETS state:** Noncoupled respiration, $J_{O_2,E}$ is
 569 maximum at optimum exogenous uncoupler concentration
 570 and phosphorylation is zero, $J_{\gg P}=0$ (See also Fig. 2).

568 respiration is observed at higher than optimum uncoupler concentrations. As a consequence of
 569 the nearly collapsed protonmotive force, the driving force is insufficient for phosphorylation
 570 and $J_{\gg P}=0$.

571 Besides the three fundamental coupling states of mitochondrial preparations, the
 572 following respiratory state also is relevant to assess respiratory function:

573 **ROX:** Residual oxygen consumption (ROX) is defined as O_2 consumption due to
 574 oxidative side reactions remaining after inhibition of the ETS. ROX is not a coupling state but
 575 represents a baseline that is used to correct mitochondrial respiration in defined coupling states

576 **(Box 3)**. ROX is not necessarily equivalent to non-mitochondrial respiration, considering
 577 oxygen-consuming reactions in mitochondria not related to ETS, such as oxygen consumption
 578 in reactions catalyzed by monoamine oxidases (type A and B), monooxygenases (cytochrome
 579 P450 monooxygenases), dioxygenase (sulfur dioxygenase and trimethyllysine dioxygenase),
 580 several hydroxylases, and more. Mitochondrial preparations, especially those obtained from
 581 liver, are contaminated by peroxisomes. This fact makes the exact determination of
 582 mitochondrial oxygen consumption and mitochondria-associated generation of reactive oxygen
 583 species complicated (Schönfeld *et al.* 2009). The dependence of ROX-linked oxygen
 584 consumption needs to be studied in detail with respect to non-ETS enzyme activities,
 585 availability of specific substrates, oxygen concentration, and electron leakage leading to the
 586 formation of reactive oxygen species.

587

588 2.3. Classical terminology for isolated mitochondria

589 *‘When a code is familiar enough, it ceases appearing like a code; one forgets that*
 590 *there is a decoding mechanism. The message is identical with its meaning’*
 591 (Hofstadter 1979).

592 Chance and Williams (1955; 1956) introduced five classical states of mitochondrial respiration
 593 and cytochrome redox states. **Table 3** shows a protocol with isolated mitochondria in a closed
 594 respirometric chamber, defining a sequence of respiratory states.

595

596 **Table 3. Metabolic states of mitochondria (Chance and**
 597 **Williams, 1956; Table V).**
 598

State	[O ₂]	ADP level	Substrate level	Respiration rate	Rate-limiting substance
1	>0	low	low	slow	ADP
2	>0	high	~0	slow	Substrate
3	>0	high	high	fast	respiratory chain
4	>0	low	high	slow	ADP
5	0	high	high	0	Oxygen

599

600 **State 1** is obtained after addition of isolated mitochondria to air-saturated
601 isoosmotic/isotonic respiration medium containing inorganic phosphate, but no fuel substrates
602 and no adenylates, *i.e.*, AMP, ADP, ATP.

603 **State 2** is induced by addition of a high concentration of ADP (typically 100 to 300 μM),
604 which stimulates respiration transiently on the basis of endogenous fuel substrates and
605 phosphorylates only a small portion of the added ADP. State 2 is then obtained at a low
606 respiratory activity limited by zero endogenous fuel substrate availability (**Table 3**). If addition
607 of specific inhibitors of respiratory complexes, such as rotenone, does not cause a further
608 decline of oxygen consumption, State 2 is equivalent to residual oxygen consumption (See
609 below). If inhibition is observed, undefined endogenous fuel substrates are a confounding factor
610 of pathway control by externally added substrates and inhibitors. In contrast to the original
611 definition, an alternative protocol is frequently applied, in which State 2 is induced by addition
612 of fuel substrate without ADP (LEAK state), followed by addition of ADP.

613 **State 3** is the state stimulated by addition of fuel substrates while the ADP concentration
614 is still high (**Table 3**) and supports coupled energy transformation through oxidative
615 phosphorylation. 'High ADP' is a concentration of ADP specifically selected to allow the
616 measurement of State 3 to State 4 transitions of isolated mitochondria in a closed respirometric
617 system. Repeated ADP titration re-establishes State 3 at 'high ADP'. Starting at oxygen
618 concentrations near air-saturation (ca. 200 μM O_2 at sea level and 37 °C), the total ADP
619 concentration added must be low enough (typically 100 to 300 μM) to allow phosphorylation
620 to ATP at a coupled oxygen consumption that does not lead to oxygen depletion during the
621 transition to State 4. In contrast, kinetically saturating ADP concentrations usually are an order
622 of magnitude higher than 'high ADP', *e.g.* 2.5 mM in isolated mitochondria. The abbreviation
623 State 3u is frequently used in bioenergetics, to indicate the state of respiration after titration of
624 an uncoupler, without sufficient emphasis on the fundamental difference between OXPHOS

625 capacity (*well-coupled* with an *endogenous* uncoupled component) and ETS capacity
626 (*noncoupled*).

627 **State 4** is a LEAK state which is obtained only if the mitochondrial preparation is intact
628 and well-coupled. Depletion of ADP by phosphorylation to ATP leads to a decline in oxygen
629 consumption in the transition from State 3 to State 4. Under these conditions, a maximum
630 protonmotive force and high ATP/ADP ratio are maintained, and the $\gg P/O_2$ ratio can be
631 calculated. State 4 respiration, L_T (**Table 1**), reflects intrinsic proton leak and intrinsic ATP
632 hydrolysis activity. Oxygen consumption in State 4 is an overestimation of LEAK respiration
633 if the contaminating ATP hydrolysis activity recycles some ATP to ADP, $J_{\ll P}$, which stimulates
634 respiration coupled to phosphorylation, $J_{\gg P} > 0$. This can be tested by inhibition of the
635 phosphorylation system using oligomycin, ensuring that $J_{\gg P} = 0$ (State 4o). Alternatively,
636 sequential ADP titrations re-establish State 3, followed by State 3 to State 4 transitions while
637 sufficient oxygen is available. However, anoxia may be reached before exhaustion of ADP
638 (State 5).

639 **State 5** is the state after exhaustion of oxygen in a closed respirometric chamber.
640 Diffusion of oxygen from the surroundings into the aqueous solution may be a confounding
641 factor preventing complete anoxia (Gnaiger 2001).

642 In **Table 3**, only States 3 and 4 (and ‘State 2’ in the alternative protocol without ADP;
643 not included in the table) are coupling control states, with the restriction that O_2 flux in State 3
644 may be limited kinetically by non-saturating ADP concentrations (**Table 1**).

645

646 2.4. Coupling states and respiratory rates

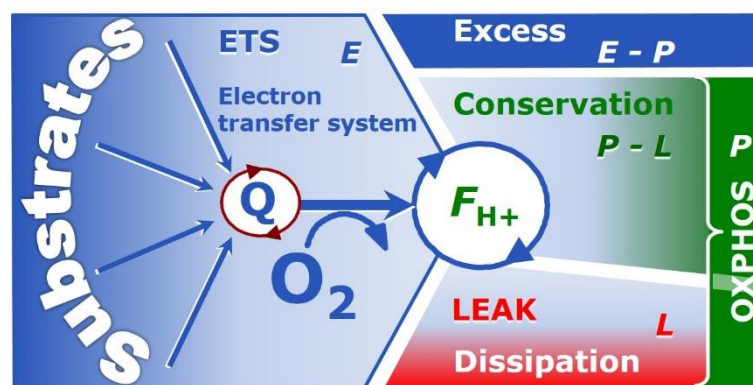
647 It is important to distinguish metabolic systems or modules from metabolic states and the
648 corresponding metabolic rates; for example: electron transfer system, ETS (**Fig. 6**), ETS state
649 (**Fig. 5**), and ETS capacity, E , respectively (**Table 1**). The protonmotive force is *high* in the
650 OXPHOS state when it drives phosphorylation, *maximum* in the LEAK state of coupled

651 mitochondria, driven by LEAK respiration at a minimum back flux of protons to the matrix
 652 side, and *very low* in the ETS state when uncouplers short-circuit the proton cycle (**Table 1**).

653

654 **Fig. 6. Four-compartment model**
 655 **of oxidative phosphorylation.**

656 Respiratory states (ETS, OXPHOS,
 657 LEAK) and corresponding rates (E ,
 658 P , L) are connected by the
 659 protonmotive force, F_{H^+} . Electron
 660 transfer system capacity, E , is



661 partitioned into the dissipative LEAK respiration, L , partial conservation of the protonmotive exergy (**Box**
 662 **4**) as the phosphorylation exergy in net OXPHOS capacity, $P-L$, and the excess capacity, $E-P$. Modified
 663 from Gnaiger (2014).

664

665 The three coupling states, ETS, LEAK and OXPHOS, are presented in a schematic
 666 context with the corresponding respiratory rates, abbreviated as E , L and P , respectively (**Fig.**
 667 **6**). This clarifies that E may exceed or be equal to P , but E cannot theoretically be lower than
 668 P . $E < P$ must be discounted as an artefact, which may be caused experimentally by: (1) loss of
 669 oxidative capacity during the time course of the respirometric assay, since E is measured
 670 subsequently to P ; (2) using too low uncoupler concentrations; (3) using high uncoupler
 671 concentrations which inhibit the ETS (Gnaiger 2008); (4) high oligomycin concentrations
 672 applied for measurement of L before titrations of uncoupler, when oligomycin exerts an
 673 inhibitory effect on E . On the other hand, the excess ETS capacity is overestimated if non-
 674 saturating $[P_i]$ or $[ADP]$ (State 3) are used.

675 $E > P$ is observed in many types of mitochondria, varying between species, tissues and cell
 676 types. It is the excess ETS capacity pushing the phosphorylation system (**Fig. 1B**) to the limit
 677 of its *capacity of utilizing* the protonmotive force. Within any type of mitochondria, the
 678 magnitude of $E > P$ depends on (1) the pathway control state with single or multiple electron

679 input into the Q-junction and involvement of three or fewer coupling sites determining the
 680 H^+_{out}/O_2 coupling stoichiometry (**Fig. 1A**); and (2) the *biochemical coupling efficiency*
 681 expressed as $(E-L)/E$, since an increase of L causes P to increase towards the limit of E . The
 682 *excess E-P capacity*, $E-P$, therefore, provides a sensitive diagnostic indicator of specific injuries
 683 of the phosphorylation system, under conditions when E remains constant but P declines
 684 relative to controls (**Fig. 6**). Substrate cocktails supporting simultaneous convergent electron
 685 transfer to the Q-junction for reconstitution of tricarboxylic acid cycle (TCA cycle) function
 686 establish pathway control states with high ETS capacity, and consequently increase the
 687 sensitivity of the $E-P$ assay.

688 When subtracting L from P , the dissipative LEAK component in the OXPHOS state may
 689 be overestimated. This can be avoided by measuring LEAK respiration in a state when the
 690 protonmotive force is adjusted to its slightly lower value in the OXPHOS state, *e.g.*, by titration
 691 of an ETS inhibitor. Any turnover-dependent components of proton leak and slip, however, are
 692 underestimated under these conditions (Garlid *et al.* 1993). In general, it is inappropriate to use
 693 the term *ATP production* for the difference of oxygen consumption measured in states P and L .
 694 The difference $P-L$ is the upper limit of the part of OXPHOS capacity that is freely available
 695 for ATP production (corrected for LEAK respiration) and is fully coupled to phosphorylation
 696 with a maximum mechanistic stoichiometry (**Fig. 6**).

697

698 **3. States and rates**

699 *3.1. The protonmotive force and proton flow*

700 The protonmotive force across the inner mitochondrial membrane (Mitchell and Moyle
 701 1967) was introduced most beautifully in the *Grey Book 1966* (see Mitchell 2011),

$$702 \quad \Delta p_{H^+} = \Delta \Psi + \Delta \mu_{H^+}/F \quad (\text{Eq. 1})$$

703 The protonmotive force consists of two partial forces: (1) The electrical part, $\Delta \Psi$, is the
 704 difference of charge (electric potential difference) and is not specific for H^+ . (2) The chemical

705 part, $\Delta\mu_{H^+}$, is the chemical potential difference in H^+ , is proportional to the pH difference, and
 706 incorporates the Faraday constant (**Table 4**).

707
 708 **Table 4. Protonmotive force and flow matrix.** Rows: Electrical and chemical
 709 isomorphic format (e and n). The Faraday constant, F , converts protonmotive force
 710 and flow from *isomorphic format* e to n . Columns: The protonmotive force is the sum
 711 of *partial isomorphic forces* F_{el} and F_{d,H^+} . In contrast to force (state), the conjugated
 712 flow (rate) cannot be partitioned.
 713

State	Force	electric	+	chemical	Unit	Notes	
Protonmotive force, e	Δp_{H^+}	= $\Delta\Psi$	+	$\Delta\mu_{H^+}/F$	$J\cdot C^{-1}$	Eq. 1e	
Chemiosmotic potential, n	$\Delta\tilde{\mu}_{H^+}$	= $\Delta\Psi\cdot F$	+	$\Delta\mu_{H^+}$	$J\cdot mol^{-1}$	Eq. 1n	
State	Isomorph e and n	Force, $F_{H^+/i}$	=	eI	+	d, H^+	
Electric charge, e		$F_{H^+/e}$	=	$F_{el/e}$	+	$F_{d,H^+/e}$	$J\cdot C^{-1}$ Eq. 2e
Amount of substance, n		$F_{H^+/n}$	=	$F_{el/n}$	+	$F_{d,H^+/n}$	$J\cdot mol^{-1}$ Eq. 2n
Rate	Isomorph e and n	Flow, $I_{H^+/i}$	=	e	or	N	
Electric charge, e		$I_{H^+/e}$		$I_{H^+/e}$			$C\cdot s^{-1}$
Amount of substance, n		$I_{H^+/n}$				$I_{H^+/n}$	$mol\cdot s^{-1}$

714
 715 Eq. 1: The Faraday constant, F , is the product of elementary charge ($e=1.602177\cdot 10^{-19}\cdot C$) and the
 716 Avogadro (Loschmidt) constant ($N_A=6.022136\cdot 10^{23}\cdot mol^{-1}$), $F=eN_A=96,485.3 C/mol$. $\Delta\tilde{\mu}_{H^+}$ is
 717 the chemiosmotic potential difference. Eqs. 1e and 1n are the classical representations of Eqs.
 718 2e and 2n.

719 Eq. 2: The protonmotive force is F_{H^+} , expressed either in isomorphic format e or n . $F_{el/e}\equiv\Delta\Psi$ is the
 720 partial protonmotive force (eI) acting generally on charged motive molecules (*i.e.* ions that are
 721 displaceable across the inner mitochondrial membrane). In contrast, $F_{d,H^+/n}\equiv\Delta\mu_{H^+}$ is the partial
 722 protonmotive force specific for proton displacement (d, H^+). The sign of the force is positive for
 723 endergonic, negative for exergonic transformations. The sign of the flow depends on the
 724 definition of the compartmental direction of the translocation (**Fig. 2**). Flow \times force = $I_{H^+/e}\cdot F_{H^+/e}$
 725 = $I_{H^+/n}\cdot F_{H^+/n}$ = Power [J/s=W].
 726

727 **Faraday constant**, $F=eN_A$ [C/mol] (**Table 4**), enables the conversion between
 728 protonmotive force, $F_{H+/e} \equiv \Delta p_{H^+}$ [J/C], expressed per *motive charge*, e [C], and protonmotive
 729 force or electrochemical potential difference, $F_{H+/n} \equiv \Delta \tilde{\mu}_{H^+} = \Delta p_{H^+} \cdot F$ [J/mol], expressed per
 730 *motive amount of protons*, n [mol]. Proton charge, e , and amount of substance, n , define the
 731 units for the isomorphic formats. Taken together, F converts protonmotive force and flow from
 732 isomorphic format e to n (Eq. 3; see also **Table 4**, Eq. 2),

$$733 \quad F_{H+/n} = F_{H+/e} \cdot eN_A \quad (\text{Eq. 3.1})$$

$$734 \quad I_{H+/n} = I_{H+/e} / (eN_A) \quad (\text{Eq. 3.2})$$

735 In each format, the protonmotive force is expressed as the sum of two partial forces. The
 736 concept expressed by the complex symbols in Eq. 1 can be explained and visualized more easily
 737 by *partial isomorphic forces* as the components of the protonmotive force:

738 **Electrical part of the protonmotive force:** (1) Isomorph e : $F_{el/e} \equiv \Delta \Psi$ is the electrical
 739 part of the protonmotive force expressed in units joule per coulomb, *i.e.* volt [V=J/C]. $F_{el/e}$ is
 740 defined as partial Gibbs energy change per *motive elementary charge*, e [C], not specific for
 741 proton charge (**Table 4**, Eq. 2e). (2) Isomorph n : $F_{el/n} \equiv \Delta \Psi \cdot F$ is the electric force expressed in
 742 units joule per mole [J/mol], defined as partial Gibbs energy change per *motive amount of*
 743 *charge*, n [mol], not specific for proton charge (**Table 4**, Eq. 2n).

744 **Chemical part of the protonmotive force:** (1) Isomorph n : $F_{d,H+/n} \equiv \Delta \mu_{H^+}$ is the chemical
 745 part (diffusion, displacement of H^+) of the protonmotive force expressed in units joule per mole
 746 [J/mol]. $F_{d,H+/n}$ is defined as partial Gibbs energy change per *motive amount of protons*, n [mol]
 747 (**Table 4**, Eq. 2n). (2) Isomorph e : $F_{d,H+/e} \equiv \Delta \mu_{H^+} / F$ is the chemical force expressed in units
 748 joule per coulomb [V], defined as partial Gibbs energy change per *motive amount of protons*
 749 *expressed in units of electric charge*, e [C], but specific for proton charge (**Table 4**, Eq. 2e).

750 Protonmotive means that there is a potential for the movement of protons, and force is a
 751 measure of the potential for motion. Motion is relative and not absolute (Principle of Galilean
 752 Relativity); likewise there is no absolute potential, but (isomorphic) forces are potential

753 differences (equations in **Table 5**). An electric partial force expressed in the format of electric
 754 charge, $F_{el/e}$, of -0.2 V (Eq. 8e) is equivalent to force in the format of amount, $F_{el,H+/n}$, of 19
 755 $\text{kJ}\cdot\text{mol}^{-1} \text{H}^+_{\text{out}}$ (Eq. 8n). For a ΔpH of 1 unit, the chemical partial force in the format of amount,
 756 $F_{d,H+/n}$, changes by $5.9 \text{kJ}\cdot\text{mol}^{-1}$ (Eq. 9n) and chemical force in the format of charge $F_{d,H+/e}$
 757 changes by 0.06 V (**Table 5**, Eq. 9e). Considering a driving force of $-470 \text{kJ}\cdot\text{mol}^{-1} \text{O}_2$ for
 758 oxidation, the thermodynamic limit of the $\text{H}^+_{\text{out}}/\text{O}_2$ ratio is reached at a value of $470/19=24$,
 759 compared to a mechanistic stoichiometry of 20 (**Fig. 1**).

760

761 **Box 4: Endergonic and exergonic transformations, exergy and dissipation**

762 A chemical reaction, or any transformation, is exergonic if the Gibbs energy change (exergy)
 763 of the reaction is negative at constant temperature and pressure. The sum of Gibbs energy
 764 changes of all internal transformations in a system can only be negative, i.e. exergy is
 765 irreversibly dissipated. Endergonic reactions are characterized by positive Gibbs energies of
 766 reaction and cannot proceed spontaneously in the forward direction as defined. For instance,
 767 the endergonic reaction »P is coupled to exergonic catabolic reactions, such that the total Gibbs
 768 energy change is negative, *i.e.* exergy must be dissipated for the reaction to proceed (**Fig. 2**).

769 In contrast, energy cannot be lost or produced in any internal process, which is the key
 770 message of the first law of thermodynamics. Thus mitochondria are the sites of energy
 771 transformation but not energy production. Open and closed systems can gain energy and exergy
 772 only by external flows, *i.e.* uptake from the environment. Exergy is the potential to perform
 773 work. In the framework of flux-force relationships (**Box 2**), the *partial* derivative of Gibbs
 774 energy per advancement of a transformation is an isomorphic force, F_{tr} (**Table 5**, Eq. 5). In
 775 other words, force is equal to exergy/motive unit (in integral form, this definition takes care of
 776 non-isothermal processes). This formal generalization represents an appreciation of the
 777 conceptual beauty of Peter Mitchell's innovation of the protonmotive force against the

778 background of the established paradigm of the electromotive force (emf) defined at the limit of
779 zero current (Cohen *et al.* 2008).

780

781 **Table 5. Power, exergy, force, flow, and advancement.**

782

Expression	Symbol	Definition	Unit	Notes
Power	P_{tr}	$P_{tr} = I_{tr} \cdot F_{tr} = \partial_{tr}G \cdot \partial t^{-1}$	$W = J \cdot s^{-1}$	Eq. 4
Force, isomorphic	F_{tr}	$F_{tr} = \partial_{tr}G \cdot \partial_{tr}\xi^{-1}$	$J \cdot x^{-1}$	Eq. 5
Flow, isomorphic	I_{tr}	$I_{tr} = d_{tr}\xi \cdot dt^{-1}$	$x \cdot s^{-1}$	Eq. 6
Advancement, n	$d_{tr}\xi_{H+/n}$	$d_{tr}\xi_{H+/n} = dn_{H+} \cdot \nu_{H+}^{-1}$	mol	Eq. 7n
Advancement, e	$d_{tr}\xi_{H+/e}$	$d_{tr}\xi_{H+/e} = de_{H+} \cdot \nu_{H+}^{-1}$	C	Eq. 7e
Electric partial force, e	$F_{el/e}$	$F_{el/e} \equiv \Delta\Psi$	V	Eq. 8e
Electric partial force, n	$F_{el/n}$	$\Delta\Psi \cdot F = 96.5 \cdot \Delta\Psi$	$kJ \cdot mol^{-1}$	Eq. 8n
Chemical partial force, e at 37 °C	$F_{d,H+/e}$	$\Delta\mu_{H+}/F = -\ln(10) \cdot RT/F \cdot \Delta pH$ $= -0.06 \cdot \Delta pH$	V $J \cdot C^{-1}$	Eq. 9e
Chemical partial force, n at 37 °C	$F_{d,H+/n}$	$\Delta\mu_{H+} = -\ln(10) \cdot RT \cdot \Delta pH$ $= -5.9 \cdot \Delta pH$	$J \cdot mol^{-1}$ $kJ \cdot mol^{-1}$	Eq. 9n

783

784 Eq. 4 to 7: An isomorphic motive entity or transformant, expressed in units x , is defined for any
785 transformation, tr . $x = mol$ or C in proton translocation. For comparison, in a mechanical,
786 vectorial advancement, $d_{me}\xi$ [m], the unit of the *force* is newton, F_{me} [$N = J \cdot m^{-1}$], and *flow* is
787 the velocity, $v = d_{me}\xi/dt$ [$m \cdot s^{-1}$], such that the flow-force product yields mechanical power,
788 P_{me} [W] (Cohen *et al.* 2008). The corresponding *vectorial flux* (flow density per area) is
789 velocity per cross-sectional area [$s^{-1} \cdot m^{-1}$]. The *scalar flux* lacks spatial information in a given
790 volume, such that flux ($m \cdot s^{-1}$ per volume [$s^{-1} \cdot m^{-2}$]) times force yields volume-specific power,
791 P_{Vme} [$W \cdot m^{-3}$].

792 Eq. 5: $\partial_{tr}G$ [J] is the partial Gibbs energy change in the advancement of transformation tr .

793 Eq. 6: For $x = C$, flow is electric current, I_{el} [$A = C \cdot s^{-1}$].

794 Eq. 7n: For a chemical reaction, the advancement of reaction r is $d_r\xi_B = d_r n_B \cdot \nu_B^{-1}$ [mol]. The
795 stoichiometric number is $\nu_B = -1$ or $\nu_B = 1$, depending on B being a product or substrate,
796 respectively, in reaction r involving one mole of B. The conjugated *intensive* molar quantity,
797 $F_{r,B} = \partial G/\partial_r \xi_B$ [$J \cdot mol^{-1}$], is the chemical force of reaction or *reaction-motive* force per

798 stoichiometric amount of B. In reaction kinetics, $d_r n_B$ is expressed as a volume-specific
 799 quantity, which is the partial contribution to the total concentration change of B, $d_r c_B = d_r n_B / V$
 800 and $d c_B = d n_B / V$, respectively. In open systems with constant volume V , $d c_B = d_r c_B + d_e c_B$,
 801 where r indicates the *internal* reaction and e indicates the *external* flux of B into the unit
 802 volume of the system. At steady state the concentration does not change, $d c_B = 0$, when $d_r c_B$
 803 is compensated for by the external flux of B, $d_r c_B = -d_e c_B$ (Gnaiger 1993b). Alternatively,
 804 $d c_B = 0$ when B is held constant by different coupled reactions in which B acts as a substrate
 805 or a product.

806 Eq. 8e: Scalar potential difference across the mitochondrial membrane. In a scalar electric
 807 transformation (flux of charge, *i.e.* current, from the matrix space to the intermembrane and
 808 extramitochondrial space) the motive force is the difference of charge. The endergonic
 809 direction of translocation is defined in **Fig. 2** as $H^+_{in} \rightarrow H^+_{out}$.

810 Eq. 8n: $F = 96.5 \text{ (kJ} \cdot \text{mol}^{-1}) / V$.

811 Eq. 9: Note that the electric partial force is independent of temperature (Eq. 8), but the chemical
 812 partial force depends on absolute temperature, T [K].

813 Eq. 9e: RT is the gas constant times absolute temperature. $\ln(10) \cdot RT / F = 59.16$ and 61.54 mV at
 814 298.15 and 310.15 K (25 and 37 °C), respectively.

815 Eq. 9n: $\ln(10) \cdot RT = 5.708$ and $5.938 \text{ kJ} \cdot \text{mol}^{-1}$ at 298.15 and 310.15 K (25 and 37 °C), respectively.

816

817 3.2. Forces and flows in physics and irreversible thermodynamics

818 According to its definition in physics, a potential difference and as such the
 819 *protonmotive force*, Δp_{H^+} , is not a force *per se* (Cohen *et al.* 2008). The fundamental forces of
 820 physics are distinguished from *motive forces* of statistical and irreversible thermodynamics.
 821 Complementary to the attempt towards unification of fundamental forces defined in physics,
 822 the concepts of Nobel laureates Lars Onsager, Erwin Schrödinger, Ilya Prigogine and Peter
 823 Mitchell (even if expressed in apparently unrelated terms) unite the diversity of *generalized* or
 824 ‘isomorphic’ *flow-force* relationships, the product of which links to the dissipation function and
 825 Second Law of thermodynamics (Schrödinger 1944; Prigogine 1967). A *motive force* is the
 826 derivative of potentially available or ‘free’ energy (exergy) per isomorphic *motive* unit (**Box 4**).

827 Perhaps the first account of a *motive force* in energy transformation can be traced back to the
828 Peripatetic school around 300 BC in the context of moving a lever, up to Newton's motive force
829 proportional to the alteration of motion (Coopersmith 2010).

830 **Vectorial and scalar forces, and fluxes:** In chemical reactions and osmotic or diffusion
831 processes occurring in a closed heterogeneous system, such as a chamber containing isolated
832 mitochondria, scalar transformations occur without measured spatial direction but between
833 separate compartments (translocation between the matrix and intermembrane space) or between
834 energetically-separated chemical substances (reactions from substrates to products). Hence, the
835 corresponding fluxes are not vectorial but scalar, and are expressed per volume and not per
836 membrane area. The corresponding motive forces are also scalar potential *differences* across
837 the membrane (**Table 5**), without taking into account the *gradients* across the 6 nm thick inner
838 mitochondrial membrane (Rich 2003).

839 **Coupling:** In energetics (ergodynamics), coupling is defined as an exergy transformation
840 fuelled by an exergonic (downhill) input process driving the advancement of an endergonic
841 (uphill) output process. The (negative) output/input power ratio is the efficiency of a coupled
842 energy transformation (**Box 2**). At the limit of maximum efficiency of a completely coupled
843 system, the (negative) input power equals the (positive) output power, such that the total power
844 approaches zero at the maximum efficiency of 1, and the process becomes fully reversible
845 without any dissipation of exergy, i.e. without entropy production.

846 **Coupled versus bound processes:** Since the chemiosmotic theory describes the
847 mechanisms of coupling in OXPHOS, it may be interesting to ask if the electrical and chemical
848 parts of proton translocation are coupled processes. This is not the case according to the
849 definition of coupling. If the coupling mechanism is disengaged, the output process becomes
850 independent of the input process, and both proceed in their downhill (exergonic) direction (**Fig.**
851 **2**). It is not possible to physically uncouple the electrical and chemical processes, which are
852 only *theoretically* partitioned as electrical and chemical components and can be measured

853 separately. If partial processes are non-separable, *i.e.*, cannot be uncoupled, then these are not
 854 *coupled* but are defined as *bound* processes. The electrical and chemical parts are tightly bound
 855 partial forces of the protonmotive force, since the flow cannot be partitioned but expressed only
 856 in either an electrical or chemical isomorphic format (**Table 4**).

857

858 **4. Normalization: flows and fluxes**

859 *4.1. Flux per chamber volume*

860 The volume-specific *flux of a chemical reaction* r is the time derivative of the
 861 advancement of the reaction per unit volume, $J_{V,B} = d_r \xi_B / dt \cdot V^{-1}$ [(mol·s⁻¹)·L⁻¹]. The *rate of*
 862 *concentration change* is dc_B/dt [(mol·L⁻¹)·s⁻¹], where concentration is $c_B = n_B/V$. It is helpful to
 863 make the subtle distinction between [mol·s⁻¹·L⁻¹] and [mol·L⁻¹·s⁻¹] for the fundamentally
 864 different quantities of volume-specific flux and rate of concentration change, which merge to a
 865 single expression only in closed systems. In open systems, external flows (such as O₂ supply)
 866 are distinguished from internal transformations (metabolic flow, O₂ consumption). In a closed
 867 system, external flows of all substances are zero and O₂ consumption (internal flow), I_{O_2}
 868 [pmol·s⁻¹], causes a decline of the amount of O₂ in the system, n_{O_2} [nmol]. Normalization of
 869 these quantities for the volume of the system, V [L=dm³], yields volume-specific O₂ flux,
 870 $J_{V,O_2} = I_{O_2}/V$ [nmol·s⁻¹·L⁻¹], and O₂ concentration, $[O_2]$ or $c_{O_2} = n_{O_2}/V$
 871 [nmol·mL⁻¹=μmol·L⁻¹=μM]. Instrumental background O₂ flux is due to external flux into a non-
 872 ideal closed respirometer, such that total volume-specific flux has to be corrected for
 873 instrumental background O₂ flux, *i.e.* O₂ diffusion into or out of the instrumental chamber. J_{V,O_2}
 874 is relevant mainly for methodological reasons and should be compared with the accuracy of
 875 instrumental resolution of background-corrected flux, *e.g.* ±1 nmol·s⁻¹·L⁻¹ (Gnaiger 2001).
 876 ‘Metabolic’ indicates O₂ flux corrected for instrumental background O₂ flux and chemical
 877 background O₂ flux due to autoxidation of chemical components added to the incubation
 878 medium.

879

880 4.2. Extensive expressions and size-specific normalization

881 Application of common and generally defined units is required for direct transfer of
 882 reported results into a database. The second [s] is the *SI* unit for the base quantity *time*. It is also
 883 the standard time-unit used in solution chemical kinetics. **Table 6** lists some conversion factors
 884 to obtain *SI* units. The term *rate* is not sufficiently defined to be useful for a database (**Fig. 7**).
 885 The inconsistency of the meanings of rate becomes fully apparent when considering Galileo
 886 Galilei's famous principle, that 'bodies of different weight all fall at the same rate (have a
 887 constant acceleration)' (Coopersmith 2010).

888 **Extensive quantities:** An extensive quantity increases proportionally with system size.
 889 The magnitude of an extensive quantity is completely additive for non-interacting subsystems,
 890 such as mass or flow expressed per defined system. The magnitude of these quantities depends
 891 on the extent or size of the system (Cohen *et al.* 2008).

892

893 **Fig. 7. Different meanings of rate**

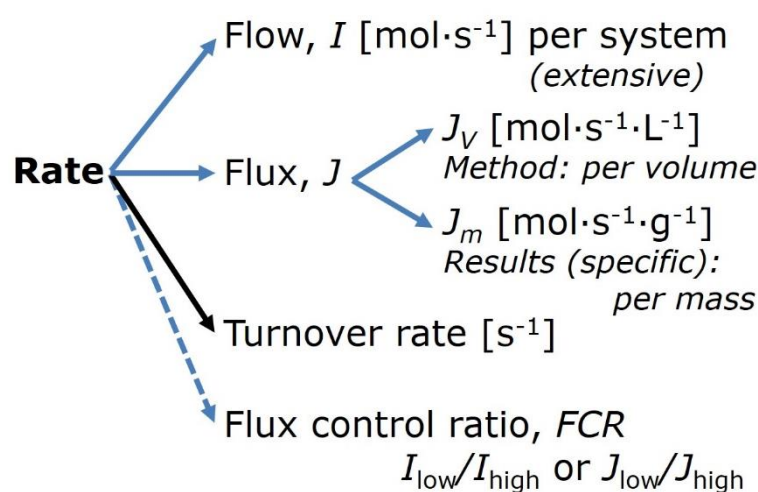
894 **may lead to confusion, if the**
 895 **normalization is not sufficiently**
 896 **specified.** Results are frequently

897 expressed as mass-specific flux, J_m ,
 898 per mg protein, dry or wet weight
 899 (mass). Cell volume, V_{cell} , or
 900 mitochondrial volume, V_{mt} , may be
 901 used for normalization (volume-

902 specific flux, $J_{V_{\text{cell}}}$ or $J_{V_{\text{mt}}}$), which then must be clearly distinguished from flux, J_v , expressed for
 903 methodological reasons per volume of the measurement system, or flow per cell, I_x .

904

905 **Size-specific quantities:** 'The adjective *specific* before the name of an extensive quantity
 906 is often used to mean *divided by mass*' (Cohen *et al.* 2008). Mass-specific flux is flow divided



907 by mass of the system. A mass-specific quantity is independent of the extent of non-interacting
 908 homogenous subsystems. Tissue-specific quantities are of fundamental interest in comparative
 909 mitochondrial physiology, where *specific* refers to the *type* rather than *mass* of the tissue. The
 910 term *specific*, therefore, must be further clarified, such that tissue mass-specific, *e.g.*, muscle
 911 mass-specific quantities are defined.

912 **Molar quantities:** ‘The adjective *molar* before the name of an extensive quantity
 913 generally means *divided by amount of substance*’ (Cohen *et al.* 2008). The notion that all molar
 914 quantities then become *intensive* causes ambiguity in the meaning of *molar Gibbs energy*. It is
 915 important to emphasize the fundamental difference between normalization for amount of
 916 substance *in a system* or for amount of motive substance *in a transformation*. When the Gibbs
 917 energy of a system, G [J], is divided by the amount of substance B in the system, n_B [mol], a
 918 *size-specific* molar quantity is obtained, $G_B = G/n_B$ [J·mol⁻¹], which is not any force at all. In
 919 contrast, when the partial Gibbs energy change, $\partial_r G$ [J], is divided by the motive amount of
 920 substance B in reaction r (advancement of reaction), $\partial_r \xi_B$ [mol], the resulting intensive molar
 921 quantity, $F_{r,B} = \partial G / \partial_r \xi_B$ [J·mol⁻¹], is the chemical motive force of reaction r involving 1 mol B
 922 (Table 5, Note to Eq. 7).

923 **Flow per system, I :** In analogy to electrical terms, flow as an extensive quantity (I ; per
 924 system) is distinguished from flux as a size-specific quantity (J ; per system size) (Fig. 7).
 925 Electric current is flow, I_{el} [A=C·s⁻¹] per system (extensive quantity). When dividing this
 926 extensive quantity by system size (membrane area), a size-specific quantity is obtained, which
 927 is electric flux (electric current density), J_{el} [A·m⁻² = C·s⁻¹·m⁻²].

928 **Size-specific flux, J :** Metabolic O₂ flow per tissue increases as tissue mass is increased.
 929 Tissue mass-specific O₂ flux should be independent of the size of the tissue sample studied in
 930 the instrument chamber, but volume-specific O₂ flux (per volume of the instrument chamber,
 931 V) should increase in direct proportion to the amount of sample in the chamber. Accurate
 932 definition of the experimental system is decisive: whether the experimental chamber is the

933 closed, open, isothermal or non-isothermal *system* with defined volume as part of the
 934 measurement apparatus, in contrast to the experimental *sample* in the chamber (**Table 6**).
 935 Volume-specific O₂ flux depends on mass-concentration of the sample in the chamber, but
 936 should be independent of the chamber volume. There are practical limitations to increasing the
 937 mass-concentration of the sample in the chamber, when one is concerned about crowding
 938 effects and instrumental time resolution.

939

940 **Table 6. Sample concentrations and normalization of flux with SI/ base units.**
 941

Expression	Symbol	Definition	SI Unit	Notes
Sample				
Identity of sample	X	Cells, animals, patients		
Number of sample entities X	N_X	Number of cells, <i>etc.</i>	x	
Mass of sample X	m_X		kg	1
Mass of entity X	M_X	$M_X = m_X \cdot N_X^{-1}$	kg·x ⁻¹	1
Mitochondria				
Mitochondria	mt	$X=mt$		
Amount of mt-elements	mte	Quantity of mt-marker	x _{mte}	
Concentrations				
Sample number concentration	C_{NX}	$C_{NX} = N_X \cdot V^{-1}$	x·m ⁻³	2
Sample mass concentration	C_{mX}	$C_{mX} = m_X \cdot V^{-1}$	kg·m ⁻³	
Mitochondrial concentration	C_{mte}	$C_{mte} = mte \cdot V^{-1}$	x _{mte} ·m ⁻³	3
Specific mitochondrial density	D_{mte}	$D_{mte} = mte \cdot m_X^{-1}$	x _{mte} ·kg ⁻¹	4
Mitochondrial content, mte per entity X	mte _X	$mte_X = mte \cdot N_X^{-1}$	x _{mte} ·x ⁻¹	5
O₂ flow and flux				
Flow	I_{O_2}	Internal flow	mol·s ⁻¹	6
Volume-specific flux	J_{V,O_2}	$J_{V,O_2} = I_{O_2} \cdot V^{-1}$	mol·s ⁻¹ ·m ⁻³	7
Flow per sample entity X	I_{X,O_2}	$I_{X,O_2} = J_{V,O_2} \cdot C_{NX}^{-1}$	mol·s ⁻¹ ·x ⁻¹	8
Mass-specific flux	J_{mX,O_2}	$J_{mX,O_2} = J_{V,O_2} \cdot C_{mX}^{-1}$	mol·s ⁻¹ ·kg ⁻¹	9
Mitochondria-specific flux	J_{mte,O_2}	$J_{mte,O_2} = J_{V,O_2} \cdot C_{mte}^{-1}$	mol·s ⁻¹ ·x _{mte} ⁻¹	10

942

943 1 The SI prefix k is used for the SI base unit of mass (kg=1,000 g). In praxis, various SI prefixes are
 944 used for convenience, to make numbers easily readable, e.g. 1 mg tissue, cell or mitochondrial mass
 945 instead of 0.000001 kg.

946 2 In case $X=cells$, the sample number concentration is $C_{Ncell}=N_{cell} \cdot V^{-1}$, and volume may be expressed
 947 in [dm³=L] or [cm³=mL]. See Table 7 for different sample types.

- 948 3 mt-concentration is an experimental variable, dependent on sample concentration: (1) $C_{mte}=mte \cdot V^{-1}$;
 949 (2) $C_{mte}=mte_X \cdot C_{NX}$; (3) $C_{mte}=C_{mX} \cdot D_{mte}$.
- 950 4 If the amount of mitochondria, mte, is expressed as mitochondrial mass, then D_{mte} is the mass
 951 fraction of mitochondria in the sample. If mte is expressed as mitochondrial volume, V_{mt} , and the
 952 mass of sample, m_X , is replaced by volume of sample, V_X , then D_{mte} is the volume fraction of
 953 mitochondria in the sample.
- 954 5 $mte_X=mte \cdot N_X^{-1}=C_{mte} \cdot C_{NX}^{-1}$.
- 955 6 Entity O_2 can be replaced by other chemical entities B to study different reactions.
- 956 7 l_{O_2} and V are defined per instrument chamber as a system of constant volume (and constant
 957 temperature), which may be closed or open. l_{O_2} is abbreviated for l_{r,O_2} , i.e. the metabolic or internal
 958 O_2 flow of the chemical reaction r in which O_2 is consumed, hence the negative stoichiometric
 959 number, $\nu_{O_2}=-1$. $l_{r,O_2}=dr_{n_{O_2}}/dt \nu_{O_2}^{-1}$. If r includes all chemical reactions in which O_2 participates, then
 960 $dr_{n_{O_2}} = dn_{O_2} - d_e n_{O_2}$, where dn_{O_2} is the change in the amount of O_2 in the instrument chamber and
 961 $d_e n_{O_2}$ is the amount of O_2 added externally to the system. At steady state, by definition $dn_{O_2}=0$, hence
 962 $dr_{n_{O_2}}=-d_e n_{O_2}$.
- 963 8 J_{V,O_2} is an experimental variable, expressed per volume of the instrument chamber.
- 964 9 l_{X,O_2} is a physiological variable, depending on the size of entity X .
- 965 10 There are many ways to normalize for a mitochondrial marker, that are used in different experimental
 966 approaches: (1) $J_{mte,O_2} = J_{V,O_2} \cdot C_{mte}^{-1}$; (2) $J_{mte,O_2} = J_{V,O_2} \cdot C_{mX}^{-1} \cdot D_{mte}^{-1} = J_{mX,O_2} \cdot D_{mte}^{-1}$; (3) $J_{mte,O_2} =$
 967 $J_{V,O_2} \cdot C_{NX}^{-1} \cdot mte_X^{-1} = l_{X,O_2} \cdot mte_X^{-1}$; (4) $J_{mte,O_2} = l_{O_2} \cdot mte^{-1}$.

969 **Sample concentration C_{mX} :** Normalization for sample concentration is required for
 970 reporting respiratory data. Consider a tissue or cells as the sample, X , and the sample mass, m_X
 971 [mg] from which a mitochondrial preparation is obtained. The sample mass is frequently
 972 measured as wet or dry weight ($m_X \equiv W_w$ or W_d [mg]), or as amount of tissue or cell protein
 973 ($m_X \equiv m_{Protein}$). In the case of permeabilized tissues, cells, and homogenates, the sample
 974 concentration, $C_{mX}=m_X/V$ [$mg \cdot mL^{-1}=g \cdot L^{-1}$], is simply the mass of the subsample of tissue that is
 975 transferred into the instrument chamber. Part of the mitochondria from the tissue is lost during
 976 preparation of isolated mitochondria, and only a fraction of mitochondria is obtained, expressed

977 as the mitochondrial yield (**Fig. 8**). At a high mitochondrial yield the sample of isolated
 978 mitochondria is more representative of the total mitochondrial population than in preparations
 979 characterized by low mitochondrial yield. Determination of the mitochondrial yield is based on
 980 measurement of the concentration of a mitochondrial marker in the tissue homogenate, $C_{\text{mte,thom}}$,
 981 which simultaneously provides information on the specific mitochondrial density in the sample
 982 (**Fig. 8**).

983

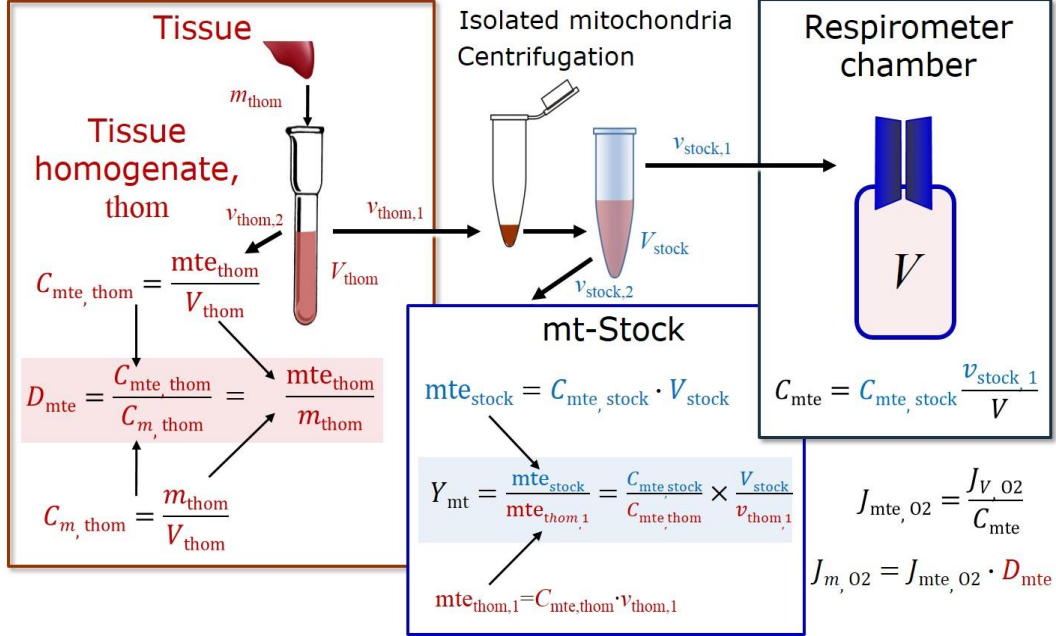
984 **Table 7. Some useful abbreviations**
 985 **of various sample types, X.**

986	<hr/>	
987	Identity of sample	X
988	<hr/>	
989	Mitochondrial preparations	mtprep
990	Isolated mitochondria	imt
991	Tissue homogenate	thom
992	Permeabilized tissue	pti
993	Permeabilized fibres	pfi
994	Permeabilized cells	pce
995	Cells	ce
996	<hr/>	
997		

998 Tissues can contain multiple cell populations which may have distinct mitochondrial
 999 subtypes. Mitochondria are also in a constant state of flux due to highly dynamic fission and
 1000 fusion cycles, and can exist in multiple stages and sizes which may be altered by a range of
 1001 factors. The isolation of mitochondria (often achieved through differential centrifugation) can
 1002 therefore yield a subsample of the mitochondrial types present in a tissue, dependent on
 1003 isolation protocols utilized (e.g. centrifugation speed). This possible artefact should be taken
 1004 into account when planning experiments using isolated mitochondria. The tendency for
 1005 mitochondria of specific sizes to be enriched at different centrifugation speeds also has the

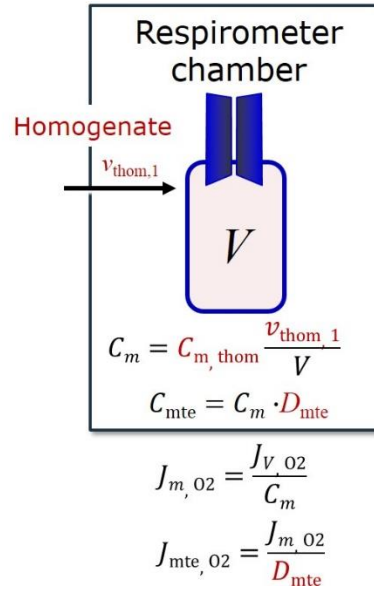
1006 potential to allow the isolation of specific mitochondrial subpopulations and therefore the
 1007 analysis of mitochondria from multiple cell lineages within a single tissue.

1008



1009

Symbol	Definition [Units]
C_{mte}	Mitochondrial concentration in chamber [$x_{mte} \cdot L^{-1}$]
C_m	Sample mass concentration in chamber [$g \cdot L^{-1}$]
D_{mte}	Specific mte-density per tissue mass [$x_{mte} \cdot g^{-1}$]
J_{m, O_2}	Mass-specific O ₂ flux [$nmol \cdot s^{-1} \cdot g^{-1}$]
J_{mte, O_2}	Mitochondria-specific O ₂ flux [$nmol \cdot s^{-1} \cdot x_{mte}^{-1}$]
mte	Amount of mitochondrial elements [x_{mte}]
m_{thom}	Mass of tissue in the homogenate [g]
Y_{mt}	Yield of isolated mitochondria



1010

1011 **Fig. 8. Normalization of volume-specific flux of isolated mitochondria and tissue**

1012 **homogenate. A:** Mitochondrial yield, Y_{mt} , in preparation of isolated mitochondria. $v_{thom,1}$

1013 and $v_{stock,1}$ are the volumes transferred from the total volume, V_{thom} and V_{stock} , respectively.

1014 $mte_{thom,1}$ is the amount of mitochondrial elements in volume $v_{thom,1}$ used for isolation. **B:**

1015 In respirometry with homogenate, $v_{thom,1}$ is transferred directly into the respirometer

1016 chamber. See **Table 6** for further explanation of symbols.

1017

1018 **Mass-specific flux, J_{mX,O_2} :** Mass-specific flux is obtained by expressing respiration per
 1019 mass of sample, m_X [mg]. X is the type of sample, *e.g.*, tissue homogenate, permeabilized fibres
 1020 or cells. Volume-specific flux is divided by mass concentration of X , $J_{mX,O_2} = J_{V,O_2}/C_{mX}$; or flow
 1021 per cell is divided by mass per cell, $J_{mcell,O_2} = I_{cell,O_2}/M_{cell}$. If mass-specific O_2 flux is constant
 1022 and independent of sample size (expressed as mass), then there is no interaction between the
 1023 subsystems. A 1.5 mg and a 3.0 mg muscle sample respire at identical mass-specific flux.
 1024 Mass-specific O_2 flux, however, may change with the mass of a tissue sample, cells or isolated
 1025 mitochondria in the measuring chamber, in which case the nature of the interaction becomes an
 1026 issue. Optimization of cell density and arrangement is generally important and particularly in
 1027 experiments carried out in wells, considering the confluency of the cell monolayer or clumps
 1028 of cells (Salabei *et al.* 2014).

1029 **Number concentration, C_{NX} :** The experimental *number concentration* of sample in the
 1030 case of cells or animals, *e.g.*, nematodes is $C_{NX} = N_X/V [X \cdot mL^{-1}]$, where N_X is the number of cells
 1031 or organisms in the chamber (**Table 6**).

1032 **Flow per sample entity, I_{X,O_2} :** A special case of normalization is encountered in
 1033 respiratory studies with permeabilized (or intact) cells. If respiration is expressed per cell, the
 1034 O_2 flow per measurement system is replaced by the O_2 flow per cell, I_{cell,O_2} (**Table 6**). O_2 flow
 1035 can be calculated from volume-specific O_2 flux, $J_{V,O_2} [nmol \cdot s^{-1} \cdot L^{-1}]$ (per V of the measurement
 1036 chamber [L]), divided by the number concentration of cells, $C_{Nce} = N_{ce}/V [cell \cdot L^{-1}]$, where N_{ce} is
 1037 the number of cells in the chamber. Cellular O_2 flow can be compared between cells of identical
 1038 size. To take into account changes and differences in cell size, further normalization is required
 1039 to obtain cell size-specific or mitochondrial marker-specific O_2 flux (Renner *et al.* 2003).

1040 The complexity changes when the sample is a whole organism studied as an experimental
 1041 model. The well-established scaling law in respiratory physiology reveals a strong interaction
 1042 of O_2 consumption and individual body mass of an organism, since *basal* metabolic rate (flow)

1043 does not increase linearly with body mass, whereas *maximum* mass-specific O₂ flux, $\dot{V}_{O_{2max}}$ or
1044 $\dot{V}_{O_{2peak}}$, is approximately constant across a large range of individual body mass (Weibel and
1045 Hoppeler 2005), with individuals, breeds, and certain species deviating substantially from this
1046 general relationship. $\dot{V}_{O_{2peak}}$ of human endurance athletes is 60 to 80 mL O₂·min⁻¹·kg⁻¹ body
1047 mass, converted to $J_{m,O_{2peak}}$ of 45 to 60 nmol·s⁻¹·g⁻¹ (Gnaiger 2014; **Table 8**).

1048

1049 *4.2. Normalization for mitochondrial content*

1050 Normalization is a problematic subject and it is essential to consider the question of the
1051 study. If the study aims to compare tissue performance, such as the effects of a certain treatment
1052 on a specific tissue, then normalization can be successful, using tissue mass or protein content,
1053 for example. If the aim, however, is to find differences of mitochondrial function independent
1054 of mitochondrial density (**Table 6**), then normalization to a mitochondrial marker is imperative.
1055 However, one cannot assume that quantitative changes in various markers such as
1056 mitochondrial proteins necessarily occur in parallel with one another. It is important to first
1057 establish that the marker chosen is not selectively altered by the performed treatment. In
1058 conclusion, the normalization must reflect the question under investigation to reach a satisfying
1059 answer. On the other hand, the goal of comparing results across projects and institutions
1060 requires some standardization on normalization for entry into a databank.

1061 **Mitochondrial concentration, C_{mte} , and mitochondrial markers:** It is important that
1062 mitochondrial content in the tissue and the measurement chamber be quantified, as a
1063 physiological output and result of mitochondrial biogenesis and degradation, and as a quantity
1064 for normalization in functional analyses. Mitochondrial organelles comprise a cellular
1065 reticulum that is in a continual flux of fusion and fission. Hence the definition of an "amount"
1066 of mitochondria is often misconceived: mitochondria cannot be counted as a number of
1067 occurring elements. Therefore, quantification of the "amount" of mitochondria depends on
1068 measurement of chosen mitochondrial markers. 'Mitochondria are the structural and functional

1069 elemental units of cell respiration' (Gnaiger 2014). The quantity of a mitochondrial marker can
 1070 be considered as the measurement of the amount of *elemental mitochondrial units* or
 1071 *mitochondrial elements*, mte. However, since mitochondrial quality changes under certain
 1072 stimuli, particularly in mitochondrial dysfunction, some markers can vary while other markers
 1073 are unchanged. (1) Mitochondrial volume or membrane area are structural markers, whereas
 1074 mitochondrial protein mass is frequently used as a marker for isolated mitochondria. (2)
 1075 Mitochondrial marker enzymes (amounts or activities) and molecular markers can be selected
 1076 as matrix markers, *e.g.*, citrate synthase activity, mtDNA; or inner mt-membrane markers, *e.g.*,
 1077 cytochrome *c* oxidase activity, *aa₃* content, cardiolipin, TOM20. (3) Extending the
 1078 measurement of mitochondrial marker enzyme activity to mitochondrial pathway capacity,
 1079 measured as ETS or OXPHOS capacity, can be considered as an integrative functional
 1080 mitochondrial marker.

1081 Depending on the type of mitochondrial marker, the mitochondrial elements, mte, are
 1082 expressed in marker-specific units. Although concentration and density are used synonymously
 1083 in physical chemistry, it is recommended to distinguish *experimental mitochondrial*
 1084 *concentration*, $C_{\text{mte}} = \text{mte}/V$ and *physiological mitochondrial density*, $D_{\text{mte}} = \text{mte}/m_X$. Then
 1085 mitochondrial density is the amount of mitochondrial elements per mass of tissue. The former
 1086 is mitochondrial density multiplied by sample mass concentration, $C_{\text{mte}} = D_{\text{mte}} \cdot C_{m_X}$, or
 1087 mitochondrial content multiplied by sample number concentration, $C_{\text{mte}} = \text{mte}_X \cdot C_{N_X}$ (**Table 6**).

1088 **Mitochondria-specific flux, $J_{\text{mte},\text{O}_2}$** : Volume-specific metabolic O₂ flux depends on: (1)
 1089 the sample concentration in the volume of the instrument chamber, C_{m_X} , or C_{N_X} ; (2) the
 1090 mitochondrial density in the sample, $D_{\text{mte}} = \text{mte}/m_X$ or $\text{mte}_X = \text{mte}/N_X$; and (3) the specific
 1091 mitochondrial activity or performance per elemental mitochondrial unit, $J_{\text{mte},\text{O}_2} = J_{V,\text{O}_2}/C_{\text{mte}}$
 1092 (**Table 6**). Obviously, the numerical results for $J_{\text{mte},\text{O}_2}$ vary according to the type of
 1093 mitochondrial marker chosen for measurement of mte and $C_{\text{mte}} = \text{mte}/V$. Some problems are
 1094 common for all mitochondrial markers: (1) Accuracy of measurement is crucial, since even a

1095 highly accurate and reproducible measurement of O₂ flux becomes inaccurate and noisy if
1096 normalized for a biased and noisy measurement of a mitochondrial marker. This problem is
1097 acute in mitochondrial respiration because the denominators used (the mitochondrial marker)
1098 are often very small moieties whose accurate and precise determination is difficult. This
1099 problem can be avoided when O₂ fluxes measured in substrate-uncoupler-inhibitor titration
1100 protocols are normalized for flux in a defined respiratory reference state, which is used as an
1101 *internal* marker and yields flux control ratios, *FCRs* (**Fig. 7**). *FCRs* are independent of any
1102 *externally* measured markers and, therefore, are statistically very robust. *FCRs* indicate
1103 qualitative changes of mitochondrial respiratory control, with highest quantitative resolution,
1104 separating the effect of mitochondrial density or concentration on J_{mX,O_2} or I_{X,O_2} from that of
1105 function per elemental mitochondrial marker, J_{mte,O_2} (Pesta *et al.* 2011; Gnaiger 2014). (2) If
1106 mitochondrial quality does not change and only the amount of mitochondria, defined by the
1107 chosen mitochondrial marker, varies as a determinant of mass-specific flux, then any marker is
1108 equally qualified and selection of the optimum marker depends only on the accuracy and
1109 precision of measurement of the mitochondrial marker. (3) If mitochondrial flux control ratios
1110 change, then there may not be any best mitochondrial marker. In general, measurement of
1111 multiple mitochondrial markers enables a comparison and evaluation of normalization for a
1112 variety of mitochondrial markers.

1113

1114 4.3. Conversion: normalization and units, for oxygen, proton and ATP flux

1115 Many different units have been used to report the rate of oxygen consumption, OCR
1116 (**Tables 8 and 9**). For studies of cells, we recommend that respiration be expressed, as far as
1117 possible, as (1) O₂ flux normalized for a mitochondrial marker, for separation of the effects of
1118 mitochondrial quality and content on cell respiration (this includes *FCRs* as a normalization for
1119 a functional mitochondrial marker); (2) O₂ flux in units of cell volume or mass, for comparison
1120 of respiration of cells with different cell size (Renner *et al.* 2003) and with studies on tissue

1121 preparations, and (3) O₂ flow in units of attomole (10⁻¹⁸ mol) of O₂ consumed by each cell in a
 1122 second [amol·s⁻¹·cell⁻¹], numerically equivalent to [pmol·s⁻¹·10⁻⁶ cells]. This convention allows
 1123 information to be easily used when designing experiments in which oxygen consumption must
 1124 be considered. For example, to estimate the volume-specific O₂ flux in an instrument chamber
 1125 that would be expected at a particular cell number concentration, one simply needs to multiply
 1126 the flow per cell by the number of cells per volume of interest. This provides the amount of O₂
 1127 [mol] consumed per time [s⁻¹] per unit volume [L⁻¹]. At an O₂ flow of 100 amol·s⁻¹·cell⁻¹ and a
 1128 cell density of 10⁹ cells·L⁻¹ (10⁶ cells·mL⁻¹), the volume-specific O₂ flux is 100 nmol·s⁻¹·L⁻¹ (100
 1129 pmol·s⁻¹·mL⁻¹). Although volume is expressed as m³ using the *SI* base unit, the litre [dm³] is the
 1130 basic unit of volume for concentration and is used for most solution chemical kinetics. If one
 1131 multiplies $I_{\text{cell},\text{O}_2}$ by $C_{N_{\text{cell}}}$, then the result will not only be the amount of O₂ [mol] consumed per
 1132 time [s⁻¹] in one litre [L⁻¹], but also the change in the concentration of oxygen per second (for
 1133 any volume of an ideally closed system). This is ideal for kinetic modeling as it blends with
 1134 chemical rate equations where concentrations are typically expressed in mol·L⁻¹ (Wagner *et al.*
 1135 2011). In studies of multinuclear cells, such as differentiated skeletal muscle cells, it is easy to
 1136 determine the number of nuclei but not the total number of cells. A generalized concept,
 1137 therefore, is obtained by substituting cells by nuclei as the sample entity. This does not hold,
 1138 however, for enucleated platelets which comprise 5% of human cells (Sender *et al.* 2016).

1139 J_{O_2} is coupled in mitochondrial steady states to proton cycling, $J_{\infty\text{H}^+} = J_{\text{H}^+\text{out}} = J_{\text{H}^+\text{in}}$ (**Fig.**
 1140 **2**). $J_{\text{H}^+\text{out}/n}$ and $J_{\text{H}^+\text{in}/n}$ [nmol·s⁻¹·L⁻¹] are converted into electrical units, $J_{\text{H}^+\text{out}/e}$
 1141 [mC·s⁻¹·L⁻¹=mA·L⁻¹] = $J_{\text{H}^+\text{out}/n}$ [nmol·s⁻¹·L⁻¹]· F [C·mol⁻¹]·10⁻⁶ (**Table 4**). At a $J_{\text{H}^+\text{out}}/J_{\text{O}_2}$ ratio or
 1142 $\text{H}^+_{\text{out}}/\text{O}_2$ of 20 ($\text{H}^+_{\text{out}}/\text{O}=10$), a volume-specific O₂ flux of 100 nmol·s⁻¹·L⁻¹ would correspond to
 1143 a proton flux of 2,000 nmol H⁺_{out}·s⁻¹·L⁻¹ or volume-specific current of 193 mA·L⁻¹.

$$1144 \quad J_{V,\text{H}^+\text{out}/e} [\text{mA}\cdot\text{L}^{-1}] = J_{V,\text{H}^+\text{out}/n} \cdot F \cdot 10^{-6} [\text{nmol}\cdot\text{s}^{-1}\cdot\text{L}^{-1}\cdot\text{mC}\cdot\text{nmol}^{-1}] \quad (\text{Eq. 10.1})$$

$$1145 \quad J_{V,\text{H}^+\text{out}/e} [\text{mA}\cdot\text{L}^{-1}] = J_{V,\text{O}_2} \cdot (\text{H}^+_{\text{out}}/\text{O}_2) \cdot F \cdot 10^{-6} [\text{mC}\cdot\text{s}^{-1}\cdot\text{L}^{-1}=\text{mA}\cdot\text{L}^{-1}] \quad (\text{Eq. 10.2})$$

1146 ETS capacity in various human cell types including HEK 293, primary HUVEC and fibroblasts
 1147 ranges from 50 to 180 $\text{amol}\cdot\text{s}^{-1}\cdot\text{cell}^{-1}$, measured in intact cells in the noncoupled state (see
 1148 Gnaiger 2014). At 100 $\text{amol}\cdot\text{s}^{-1}\cdot\text{cell}^{-1}$ corrected for ROX (corresponding to a catabolic power
 1149 of $-48 \text{ pW}\cdot\text{cell}^{-1}$), the current across the mt-membranes, I_e , approximates 193 $\text{pA}\cdot\text{cell}^{-1}$ or 0.2
 1150 nA per cell. See Rich (2003) for an extension of quantitative bioenergetics from the molecular
 1151 to the human scale, with a transmembrane proton flux equivalent to 520 A in an adult at a
 1152 catabolic power of -110 W . Modelling approaches illustrate the link between proton motive
 1153 force and currents (Willis *et al.* 2016).

1154

1155 **Table 8. Conversion of various units used in respirometry and**
 1156 **ergometry.** e is the number of electrons or reducing equivalents. z_B is the
 1157 charge number of entity B.

1158

1 Unit	x	Multiplication factor	SI-Unit	Note
$\text{ng}\cdot\text{atom O}\cdot\text{s}^{-1}$	(2 e)	0.5	$\text{nmol O}_2\cdot\text{s}^{-1}$	
$\text{ng}\cdot\text{atom O}\cdot\text{min}^{-1}$	(2 e)	8.33	$\text{pmol O}_2\cdot\text{s}^{-1}$	
$\text{natom O}\cdot\text{min}^{-1}$	(2 e)	8.33	$\text{pmol O}_2\cdot\text{s}^{-1}$	
$\text{nmol O}_2\cdot\text{min}^{-1}$	(4 e)	16.67	$\text{pmol O}_2\cdot\text{s}^{-1}$	
$\text{nmol O}_2\cdot\text{h}^{-1}$	(4 e)	0.2778	$\text{pmol O}_2\cdot\text{s}^{-1}$	
$\text{mL O}_2\cdot\text{min}^{-1}$ at STPD ^a		0.744	$\mu\text{mol O}_2\cdot\text{s}^{-1}$	1
$\text{W} = \text{J/s}$ at -470 kJ/mol O_2		-2.128	$\mu\text{mol O}_2\cdot\text{s}^{-1}$	
$\text{mA} = \text{mC}\cdot\text{s}^{-1}$	($z_{\text{H}^+}=1$)	10.36	$\text{nmol H}^+\cdot\text{s}^{-1}$	2
$\text{mA} = \text{mC}\cdot\text{s}^{-1}$	($z_{\text{O}_2}=4$)	2.59	$\text{nmol O}_2\cdot\text{s}^{-1}$	2
$\text{nmol H}^+\cdot\text{s}^{-1}$	($z_{\text{H}^+}=1$)	0.09649	mA	3
$\text{nmol O}_2\cdot\text{s}^{-1}$	($z_{\text{O}_2}=4$)	0.38594	mA	3

1159 1 At standard temperature and pressure dry (STPD: $0 \text{ }^\circ\text{C}=273.15 \text{ K}$ and 1

1160 $\text{atm}=101.325 \text{ kPa}=760 \text{ mmHg}$), the molar volume of an ideal gas, V_m , and V_{m,O_2}

1161 is 22.414 and 22.392 $\text{L}\cdot\text{mol}^{-1}$ respectively. Rounded to three decimal places, both

1162 values yield the conversion factor of 0.744. For comparison at NTPD ($20 \text{ }^\circ\text{C}$),

1163 V_{m,O_2} is 24.038 $\text{L}\cdot\text{mol}^{-1}$. Note that the SI standard pressure is 100 kPa.

1164 2 The multiplication factor is $10^6/(z_B\cdot F)$.

1165 3 The multiplication factor is $z_B \cdot F/10^6$.

1166

1167

Table 9. Conversion for units with preservation of numerical values.

Name	Frequently used unit	Equivalent unit	Note
Volume-specific flux, J_{V,O_2}	$\text{pmol} \cdot \text{s}^{-1} \cdot \text{mL}^{-1}$ $\text{mmol} \cdot \text{s}^{-1} \cdot \text{L}^{-1}$	$\text{nmol} \cdot \text{s}^{-1} \cdot \text{L}^{-1}$ $\text{mol} \cdot \text{s}^{-1} \cdot \text{m}^{-3}$	1
Cell-specific flow, I_{O_2}	$\text{pmol} \cdot \text{s}^{-1} \cdot 10^{-6} \text{ cells}$ $\text{pmol} \cdot \text{s}^{-1} \cdot 10^{-9} \text{ cells}$	$\text{amol} \cdot \text{s}^{-1} \cdot \text{cell}^{-1}$ $\text{zmol} \cdot \text{s}^{-1} \cdot \text{cell}^{-1}$	2 3
Cell number concentration, C_{Nce}	$10^6 \text{ cells} \cdot \text{mL}^{-1}$	$10^9 \text{ cells} \cdot \text{L}^{-1}$	
Mitochondrial protein concentration, C_{mte}	$0.1 \text{ mg} \cdot \text{mL}^{-1}$	$0.1 \text{ g} \cdot \text{L}^{-1}$	
Mass-specific flux, J_{m,O_2}	$\text{pmol} \cdot \text{s}^{-1} \cdot \text{mg}^{-1}$	$\text{nmol} \cdot \text{s}^{-1} \cdot \text{g}^{-1}$	4
Catabolic power, P_{k,O_2}	$\mu\text{W} \cdot 10^{-6} \text{ cells}$	$\text{pW} \cdot \text{cell}^{-1}$	1
Volume	1,000 L L mL μL fL	m^3 (1,000 kg) dm^3 (kg) cm^3 (g) mm^3 (mg) μm^3 (pg)	
Amount of substance concentration	$\text{M} = \text{mol} \cdot \text{L}^{-1}$	$\text{mol} \cdot \text{dm}^{-3}$	

1168

1169 1 pmol: picomole = 10^{-12} mol

1170 2 amol: attomole = 10^{-18} mol

1171 3 zmol: zeptomole = 10^{-21} mol

1172 4 nmol: nanomole = 10^{-9} mol

1173

1174 For NADH- and succinate-linked respiration, the mechanistic »P/O₂ ratio (referring to the

1175 full 4 electron reduction of O₂) is calculated at 20/3.7 and 12/3.7, respectively (Eq. 11) equal to

1176 5.4 and 3.3. The classical »P/O ratios (referring to the 2 electron reduction of 0.5 O₂) are 2.7

1177 and 1.6 (Watt *et al.* 2010), in direct agreement with the measured »P/O ratio for succinate of

1178 1.58 ± 0.02 (Gnaiger *et al.* 2000; for detailed reviews see Wikström and Hummer 2012;

1179 Sazanov 2015),

$$1180 \quad \gg\text{P/O}_2 = (\text{H}^+_{\text{out}}/\text{O}_2)/(\text{H}^+_{\text{in}}/\gg\text{P}) \quad (11)$$

1181 In summary (**Fig. 1**),

$$1182 \quad J_{V,\gg\text{P}} [\text{nmol} \cdot \text{s}^{-1} \cdot \text{L}^{-1}] = J_{V,\text{O}_2} \cdot (\text{H}^+_{\text{out}}/\text{O}_2)/(\text{H}^+_{\text{in}}/\gg\text{P}) \quad (12.1)$$

$$1183 \quad J_{V,\gg\text{P}} [\text{nmol} \cdot \text{s}^{-1} \cdot \text{L}^{-1}] = J_{V,\text{O}_2} \cdot (\gg\text{P/O}_2) \quad (12.2)$$

1184 We consider isolated mitochondria as powerhouses and proton pumps as molecular machines

1185 to relate experimental results to energy metabolism of the intact cell. The cellular »P/O₂ based

1186 on oxidation of glycogen is increased by the glycolytic (fermentative) substrate-level
1187 phosphorylation of 3 »P/Glyc, *i.e.*, 0.5 mol »P for each mol O₂ consumed in the complete
1188 oxidation of a mol glycosyl unit (Glyc). Adding 0.5 to the mitochondrial »P/O₂ ratio of 5.4
1189 yields a bioenergetic cell physiological »P/O₂ ratio close to 6. Two NADH equivalents are
1190 formed during glycolysis and transported from the cytosol into the mitochondrial matrix, either
1191 by the malate-aspartate shuttle or by the glycerophosphate shuttle resulting in different
1192 theoretical yield of ATP generated by mitochondria, the energetic cost of which potentially
1193 must be taken into account. Considering also substrate-level phosphorylation in the TCA cycle,
1194 this high »P/O₂ ratio not only reflects proton translocation and OXPHOS studied in isolation,
1195 but integrates mitochondrial physiology with energy transformation in the living cell (Gnaiger
1196 1993a).

1197 For an overall perspective of mitochondrial physiology, we may link cellular
1198 bioenergetics to systemic human respiratory activity, addressing cell- and tissue-specific
1199 mitochondrial function as the next step. An O₂ flow of 234 μmol·s⁻¹ per individual or flux of
1200 3.3 nmol·s⁻¹·g⁻¹ body mass corresponds to -110 W catabolic energy flow at a body mass of 70
1201 kg and -470 kJ/mol O₂. Considering a cell count of 514·10⁶ to 646·10⁶ cells per g cell mass
1202 (Sender *et al.* 2016; Ahluwalia 2017), the average O₂ flow per cell at J_{m,O_2peak} of 45 nmol·s⁻¹·g⁻¹
1203 (60 mL O₂·min⁻¹·kg⁻¹) is 88 amol·s⁻¹·cell⁻¹, which compares well with OXPHOS capacity of
1204 human fibroblasts (Gnaiger 2014). We can describe our bodies as the sum of 30·10¹² human
1205 cells (30 trillion) and 38·10¹² microbial cells; Sender *et al.* 2016). At 5 L of blood and 5·10¹²
1206 erythrocytes/L, the number of red blood cells not containing mitochondria is 25·10¹² or 84%
1207 compared to the total number of mitochondria-containing cells of 6·10¹² (Sender *et al.* 2016).
1208 An estimate of mitochondrial content at 300 mitochondria per cell (West *et al.* 2002) raises
1209 questions on the concept of mitochondrial ‘number’ (90-680 per cell; Robin and Wong 1988).
1210 Cell count is controversial in the case of multinuclear muscle cells, which contribute 43% to
1211 the total cell mass of a reference man of 70 kg total body mass. Subtracting 25% extracellular

1212 fluid and 7% extracellular solids, a cell mass of 46 kg is obtained, of which 20 kg is myocytes
1213 and 13 kg is adipocytes. If the total number of mitochondria is $2 \cdot 10^{15}$ (2 quadrillion mt or 300
1214 mitochondria $\times 6 \cdot 10^{12}$ of cells containing mitochondria), mitochondrial fitness is indicated if
1215 O_2 flow of $0.1 \text{ amol} \cdot \text{s}^{-1} \cdot \text{mt}^{-1}$ at rest can be activated to $1.7 \text{ amol} \cdot \text{s}^{-1} \cdot \text{mt}^{-1}$ at high ergometric
1216 performance. {*EG: These numbers must be re-examined, on the basis of nuclei per muscle cells*
1217 *mass. Please, consider these figures as they are now merely as an illustration of the rationale,*
1218 *not as final calculations at all. Any critical input is highly welcome.*}

1219

1220 **5. Conclusions**

1221 MitoEAGLE can serve as a gateway to better diagnose mitochondrial respiratory defects
1222 linked to genetic variation, age-related health risks, sex-specific mitochondrial performance,
1223 lifestyle with its effects on degenerative diseases, and thermal and chemical environment. The
1224 present recommendations on coupling control states and rates, linked to the concept of the
1225 protonmotive force (Part 1) will be extended in a series of manuscripts on pathway control of
1226 mitochondrial respiration, respiratory states in intact cells, and harmonization of experimental
1227 procedures.

1228 The optimal choice for expressing O_2 flow per biological system, and normalization for
1229 specific tissue-markers (volume, mass, protein) and mitochondrial markers (volume, protein,
1230 content, mtDNA, activity of marker enzymes, respiratory reference state) is guided by the
1231 scientific question. Interpretation of the obtained data depends critically on appropriate
1232 normalization, and therefore reporting rates merely as $\text{nmol} \cdot \text{s}^{-1}$ is discouraged, since it restricts
1233 the analysis to intra-experimental comparison of relative (qualitative) differences. Expressing
1234 O_2 consumption per cell may not be possible when dealing with tissues. For studies with
1235 mitochondrial preparations, we recommend that normalizations be provided as far as possible:
1236 (1) on a per cell basis as O_2 flow (a biophysical normalization); (2) per g cell or tissue protein,
1237 or per cell or tissue mass as mass-specific O_2 flux (a cellular normalization); and (3) per

1238 mitochondrial marker as mt-specific flux (a mitochondrial normalization). With information on
1239 cell size and the use of multiple normalizations, maximum potential information is available
1240 (Renner *et al.* 2003; Wagner *et al.* 2011; Gnaiger 2014). When using isolated mitochondria,
1241 mitochondrial protein is a frequently applied mitochondrial marker, the use of which is basically
1242 restricted to isolated mitochondria. Mitochondrial markers, such as citrate synthase activity as
1243 an enzymatic matrix marker, provide a link to the tissue of origin on the basis of calculating the
1244 mitochondrial yield, *i.e.*, the fraction of mitochondrial marker obtained from a unit mass of
1245 tissue.

1246

1247 **Acknowledgements**

1248 We thank M. Beno for management assistance. Supported by COST Action CA15203
1249 MitoEAGLE and K-Regio project MitoFit (EG).

1250 **Competing financial interests:** E.G. is founder and CEO of Oroboros Instruments, Innsbruck,
1251 Austria.

1252

1253 **6. References** (*incomplete; www links will be deleted in the final version*)

1254 Ahluwalia A. Allometric scaling in-vitro. *Sci Rep* 2017;7:42113.

1255 Altmann R. Die Elementarorganismen und ihre Beziehungen zu den Zellen. Zweite vermehrte

1256 Auflage. Verlag Von Veit & Comp, Leipzig 1894;160 pp. -

1257 www.mitoeagle.org/index.php/Altmann_1894_Verlag_Von_Veit_%26_Comp

1258 Birkedal R, Laasmaa M, Vendelin M. The location of energetic compartments affects

1259 energetic communication in cardiomyocytes. *Front Physiol* 2014;5:376. doi:

1260 10.3389/fphys.2014.00376. eCollection 2014. PMID: 25324784

1261 Brown GC. Control of respiration and ATP synthesis in mammalian mitochondria and cells.

1262 *Biochem J* 1992;284:1-13. - www.mitoeagle.org/index.php/Brown_1992_Biochem_J

- 1263 Chance B, Williams GR. Respiratory enzymes in oxidative phosphorylation: III. The steady
1264 state. J Biol Chem 1955;217:409-27. -
1265 www.mitoeagle.org/index.php/Chance_1955_J_Biol_Chem-III
- 1266 Chance B, Williams GR. Respiratory enzymes in oxidative phosphorylation. IV. The
1267 respiratory chain. J Biol Chem 1955;217:429-38. -
1268 www.mitoeagle.org/index.php/Chance_1955_J_Biol_Chem-IV
- 1269 Chance B, Williams GR. The respiratory chain and oxidative phosphorylation. Adv Enzymol
1270 Relat Subj Biochem 1956;17:65-134. -
1271 www.mitoeagle.org/index.php/Chance_1956_Adv_Enzymol_Relat_Subj_Biochem
- 1272 Cohen ER, Cvitas T, Frey JG, Holmström B, Kuchitsu K, Marquardt R, Mills I, Pavese F,
1273 Quack M, Stohner J, Strauss HL, Takami M, Thor HL. Quantities, Units and Symbols
1274 in Physical Chemistry, IUPAC Green Book 2008;3rd Edition, 2nd Printing, IUPAC &
1275 RSC Publishing, Cambridge. -
1276 www.mitoeagle.org/index.php/Cohen_2008_IUPAC_Green_Book
- 1277 Coopersmith J. Energy, the subtle concept. The discovery of Feynman's blocks from Leibnitz
1278 to Einstein. Oxford University Press 2010;400 pp.
- 1279 Dai Q, Shah AA, Garde RV, Yonish BA, Zhang L, Medvitz NA, Miller SE, Hansen EL, Dunn
1280 CN, Price TM. A truncated progesterone receptor (PR-M) localizes to the
1281 mitochondrion and controls cellular respiration. ???
- 1282 Dufour S, Rouse N, Canioni P, Diolez P. Top-down control analysis of temperature effect on
1283 oxidative phosphorylation. Biochem J 1996;314:743-51.
- 1284 Ernster L, Schatz G Mitochondria: a historical review. J Cell Biol 1981;91:227s-55s. -
1285 www.mitoeagle.org/index.php/Ernster_1981_J_Cell_Biol
- 1286 Estabrook RW. Mitochondrial respiratory control and the polarographic measurement of
1287 ADP:O ratios. Methods Enzymol 1967;10:41-7. -
1288 www.mitoeagle.org/index.php/Estabrook_1967_Methods_Enzymol

- 1289 Fell D. Understanding the control of metabolism. Portland Press 1997.
- 1290 Garlid KD, Semrad C, Zinchenko V. Does redox slip contribute significantly to mitochondrial
1291 respiration? In: Schuster S, Rigoulet M, Ouhabi R, Mazat J-P (eds) Modern trends in
1292 biothermokinetics. Plenum Press, New York, London 1993;287-93.
- 1293 Gerö D, Szabo C. Glucocorticoids suppress mitochondrial oxidant production via
1294 upregulation of uncoupling protein 2 in hyperglycemic endothelial cells. PLoS One
1295 2016;11:e0154813.
- 1296 Gnaiger E. Efficiency and power strategies under hypoxia. Is low efficiency at high glycolytic
1297 ATP production a paradox? In: Surviving Hypoxia: Mechanisms of Control and
1298 Adaptation. Hochachka PW, Lutz PL, Sick T, Rosenthal M, Van den Thillart G (eds.)
1299 CRC Press, Boca Raton, Ann Arbor, London, Tokyo 1993a:77-109. -
1300 www.mitoeagle.org/index.php/Gnaiger_1993_Hypoxia
- 1301 Gnaiger E. Nonequilibrium thermodynamics of energy transformations. Pure Appl Chem
1302 1993b;65:1983-2002. - www.mitoeagle.org/index.php/Gnaiger_1993_Pure_Appl_Chem
- 1303 Gnaiger E. Bioenergetics at low oxygen: dependence of respiration and phosphorylation on
1304 oxygen and adenosine diphosphate supply. Respir Physiol 2001;128:277-97. -
1305 www.mitoeagle.org/index.php/Gnaiger_2001_Respir_Physiol
- 1306 Gnaiger E. Mitochondrial pathways and respiratory control. An introduction to OXPHOS
1307 analysis. 4th ed. Mitochondr Physiol Network 2014;19.12. Oroboros MiPNet
1308 Publications, Innsbruck:80 pp. -
1309 www.mitoeagle.org/index.php/Gnaiger_2014_MitoPathways
- 1310 Gnaiger E. Capacity of oxidative phosphorylation in human skeletal muscle. New
1311 perspectives of mitochondrial physiology. Int J Biochem Cell Biol 2009;41:1837-45. -
1312 www.mitoeagle.org/index.php/Gnaiger_2009_Int_J_Biochem_Cell_Biol
- 1313 Gnaiger E, Méndez G, Hand SC. High phosphorylation efficiency and depression of
1314 uncoupled respiration in mitochondria under hypoxia. Proc Natl Acad Sci USA

- 1315 2000;97:11080-5. -
- 1316 www.mitoeagle.org/index.php/Gnaiger_2000_Proc_Natl_Acad_Sci_U_S_A
- 1317 Hofstadter DR. Gödel, Escher, Bach: An eternal golden braid. A metaphorical fugue on minds
1318 and machines in the spirit of Lewis Carroll. Harvester Press 1979;499 pp. -
- 1319 www.mitoeagle.org/index.php/Hofstadter_1979_Harvester_Press
- 1320 Illaste A, Laasmaa M, Peterson P, Vendelin M. Analysis of molecular movement reveals
1321 latticelike obstructions to diffusion in heart muscle cells. *Biophys J* 2012;102:739-48. -
1322 PMID: 22385844
- 1323 Jepihhina N, Beraud N, Sepp M, Birkedal R, Vendelin M. Permeabilized rat cardiomyocyte
1324 response demonstrates intracellular origin of diffusion obstacles. *Biophys J*
1325 2011;101:2112-21. - PMID: 22067148
- 1326 Komlódi T, Tretter L. Methylene blue stimulates substrate-level phosphorylation catalysed by
1327 succinyl-CoA ligase in the citric acid cycle. *Neuropharmacology* 2017;123:287-98. -
1328 www.mitoeagle.org/index.php/Komlodi_2017_Neuropharmacology
- 1329 Lee SR, Kim HK, Song IS, Youm J, Dizon LA, Jeong SH, Ko TH, Heo HJ, Ko KS, Rhee BD,
1330 Kim N, Han J. Glucocorticoids and their receptors: insights into specific roles in
1331 mitochondria. *Prog Biophys Mol Biol* 2013;112:44-54.
- 1332 Lemieux H, Blier PU, Gnaiger E. Remodeling pathway control of mitochondrial respiratory
1333 capacity by temperature in mouse heart: electron flow through the Q-junction in
1334 permeabilized fibers. *Sci Rep* 2017;7:2840. -
1335 www.mitoeagle.org/index.php/Lemieux_2017_Sci_Rep
- 1336 Lenaz G, Tioli G, Falasca AI, Genova ML. Respiratory supercomplexes in mitochondria. In:
1337 Mechanisms of primary energy trasduction in biology. M Wikstrom (ed) Royal Society
1338 of Chemistry Publishing, London, UK 2017:296-337 (in press)
- 1339 Margulis L. Origin of eukaryotic cells. New Haven: Yale University Press 1970.

- 1340 Meinild Lundby AK, Jacobs RA, Gehrig S, de Leur J, Hauser M, Bonne TC, Flück D,
1341 Dandanell S, Kirk N, Kaech A, Ziegler U, Larsen S, Lundby C. Exercise training
1342 increases skeletal muscle mitochondrial volume density by enlargement of existing
1343 mitochondria and not de novo biogenesis. *Acta Physiol (Oxf)* 2017;[Epub ahead of
1344 print].
- 1345 Miller GA. *The science of words*. Scientific American Library New York 1991;276 pp. -
1346 www.mitoeagle.org/index.php/Miller_1991_Scientific_American_Library
- 1347 Mitchell P. Chemiosmotic coupling in oxidative and photosynthetic phosphorylation *Biochim*
1348 *Biophys Acta Bioenergetics* 2011;1807:1507-38. -
1349 <http://www.sciencedirect.com/science/article/pii/S0005272811002283>
- 1350 Mitchell P, Moyle J. Respiration-driven proton translocation in rat liver mitochondria.
1351 *Biochem J* 1967;105:1147-62. -
1352 www.mitoeagle.org/index.php/Mitchell_1967_Biochem_J
- 1353 Moreno M, Giacco A, Di Munno C, Goglia F. Direct and rapid effects of 3,5-diiodo-L-
1354 thyronine (T2). *Mol Cell Endocrinol* 2017;7207:30092-8.
- 1355 Morrow RM, Picard M, Derbeneva O, Leipzig J, McManus MJ, Gousspillou G, Barbat-Artigas
1356 S, Dos Santos C, Hepple RT, Murdock DG, Wallace DC. Mitochondrial energy
1357 deficiency leads to hyperproliferation of skeletal muscle mitochondria and enhanced
1358 insulin sensitivity. *Proc Natl Acad Sci U S A* 2017;114:2705-10. -
1359 www.mitoeagle.org/index.php/Morrow_2017_Proc_Natl_Acad_Sci_U_S_A
- 1360 Nicholls DG, Ferguson S. *Bioenergetics 4*. Elsevier 2013.
- 1361 Paradies G, Paradies V, De Benedictis V, Ruggiero FM, Petrosillo G. Functional role of
1362 cardiolipin in mitochondrial bioenergetics. *Biochim Biophys Acta* 2014;1837:408-17. -
1363 http://www.mitoeagle.org/index.php/Paradies_2014_Biochim_Biophys_Acta
- 1364 Price TM, Dai Q. The Role of a Mitochondrial Progesterone Receptor (PR-M) in
1365 Progesterone Action. *Semin Reprod Med.* 2015;33:185-94.

- 1366 Prigogine I. Introduction to thermodynamics of irreversible processes. Interscience, New
1367 York, 1967;3rd ed.
- 1368 Puchowicz MA, Varnes ME, Cohen BH, Friedman NR, Kerr DS, Hoppel CL. Oxidative
1369 phosphorylation analysis: assessing the integrated functional activity of human skeletal
1370 muscle mitochondria – case studies. *Mitochondrion* 2004;4:377-85. -
1371 www.mitoeagle.org/index.php/Puchowicz_2004_Mitochondrion
- 1372 P. M. Quiros, A. Mottis, and J. Auwerx. Mitonuclear communication in homeostasis and
1373 stress. *Nat Rev Mol Cell Biol* 2016;17:213-26.
- 1374 Renner K, Amberger A, Konwalinka G, Gnaiger E. Changes of mitochondrial respiration,
1375 mitochondrial content and cell size after induction of apoptosis in leukemia cells.
1376 *Biochim Biophys Acta* 2003;1642:115-23. -
1377 www.mitoeagle.org/index.php/Renner_2003_Biochim_Biophys_Acta
- 1378 Rich P. Chemiosmotic coupling: The cost of living. *Nature* 2003;421:583. -
1379 www.mitoeagle.org/index.php/Rich_2003_Nature
- 1380 Robin ED, Wong R. Mitochondrial DNA molecules and virtual number of mitochondria per
1381 cell in mammalian cells. *J Cell Physiol* 1988;136:507-13.
- 1382 Rostovtseva TK, Sheldon KL, Hassanzadeh E, Monge C, Saks V, Bezrukov SM, Sackett DL.
1383 Tubulin binding blocks mitochondrial voltage-dependent anion channel and regulates
1384 respiration. *Proc Natl Acad Sci USA* 2008;105:18746-51. -
1385 www.mitoeagle.org/index.php/Rostovtseva_2008_Proc_Natl_Acad_Sci_U_S_A
- 1386 Rustin P, Parfait B, Chretien D, Bourgeron T, Djouadi F, Bastin J, Rötig A, Munnich A.
1387 Fluxes of nicotinamide adenine dinucleotides through mitochondrial membranes in
1388 human cultured cells. *J Biol Chem* 1996;271:14785-90.
- 1389 Saks VA, Veksler VI, Kuznetsov AV, Kay L, Sikk P, Tiivel T, Tranqui L, Olivares J, Winkler
1390 K, Wiedemann F, Kunz WS. Permeabilised cell and skinned fiber techniques in studies

- 1391 of mitochondrial function in vivo. Mol Cell Biochem 1998;184:81-100. -
- 1392 http://www.mitoeagle.org/index.php/Saks_1998_Mol_Cell_Biochem
- 1393 Salabei JK, Gibb AA, Hill BG. Comprehensive measurement of respiratory activity in
- 1394 permeabilized cells using extracellular flux analysis. Nat Protoc 2014;9:421-38.
- 1395 Sazanov LA. A giant molecular proton pump: structure and mechanism of respiratory
- 1396 complex I. Nat Rev Mol Cell Biol 2015;16:375-88. -
- 1397 www.mitoeagle.org/index.php/Sazanov_2015_Nat_Rev_Mol_Cell_Biol
- 1398 Schönfeld P, Dymkowska D, Wojtczak L. Acyl-CoA-induced generation of reactive oxygen
- 1399 species in mitochondrial preparations is due to the presence of peroxisomes. Free Radic
- 1400 Biol Med 2009;47:503-9.
- 1401 Schrödinger E. What is life? The physical aspect of the living cell. Cambridge Univ Press,
- 1402 1944. - www.mitoeagle.org/index.php/Gnaiger_1994_BTK
- 1403 Sender R, Fuchs S, Milo R. Revised estimates for the number of human and bacteria cells in
- 1404 the body. PLoS Biol 2016;14:e1002533.
- 1405 Simson P, Jepihhina N, Laasmaa M, Peterson P, Birkedal R, Vendelin M. Restricted ADP
- 1406 movement in cardiomyocytes: Cytosolic diffusion obstacles are complemented with a
- 1407 small number of open mitochondrial voltage-dependent anion channels. J Mol Cell
- 1408 Cardiol 2016;97:197-203. - PMID: 27261153
- 1409 Stucki JW, Ineichen EA. Energy dissipation by calcium recycling and the efficiency of
- 1410 calcium transport in rat-liver mitochondria. Eur J Biochem 1974;48:365-75.
- 1411 Wagner BA, Venkataraman S, Buettner GR. The rate of oxygen utilization by cells. Free
- 1412 Radic Biol Med. 2011;51:700-712.
- 1413 <http://dx.doi.org/10.1016/j.freeradbiomed.2011.05.024> PMID: PMC3147247
- 1414 Watt IN, Montgomery MG, Runswick MJ, Leslie AG, Walker JE. Bioenergetic cost of
- 1415 making an adenosine triphosphate molecule in animal mitochondria. Proc Natl Acad Sci

- 1416 U S A 2010;107:16823-7. -
- 1417 www.mitoeagle.org/index.php/Watt_2010_Proc_Natl_Acad_Sci_U_S_A
- 1418 Weibel ER, Hoppeler H. Exercise-induced maximal metabolic rate scales with muscle aerobic
1419 capacity. J Exp Biol 2005;208:1635–44.
- 1420 West GB, Woodruff WH, Brown JH. Allometric scaling of metabolic rate from molecules and
1421 mitochondria to cells and mammals. Proc Natl Acad Sci USA 2002;99 Suppl 1:2473–8.
- 1422 Wikström M, Hummer G. Stoichiometry of proton translocation by respiratory complex I and
1423 its mechanistic implications. Proc Natl Acad Sci U S A 2012;109:4431-6. -
- 1424 www.mitoeagle.org/index.php/Wikstroem_2012_Proc_Natl_Acad_Sci_U_S_A
- 1425 Willis WT, Jackman MR, Messer JI, Kuzmiak-Glancy S, Glancy B. A simple hydraulic
1426 analog model of oxidative phosphorylation. Med Sci Sports Exerc. 2016;48:990-1000.
- 1427

1428 **Supplement**

1429

1430
1431**Table S1. SI prefixes (IUPAC).**

Submultiple	Prefix	Symbol	Multiple	Prefix	Symbol
10^{-3}	milli	m	10^3	kilo	k
10^{-6}	micro	μ	10^6	mega	M
10^{-9}	nano	n	10^9	giga	G
10^{-12}	pico	p	10^{12}	tera	T
10^{-15}	femto	f	10^{15}	peta	P
10^{-18}	atto	a	10^{18}	exa	E
10^{-21}	zepto	z	10^{21}	zetta	Z

1432